Continental Shelf Research 30 (2010) 1226–1240

Contents lists available at ScienceDirect

Continental Shelf Research

journal homepage: www.elsevier.com/locate/csr

Understanding impacts of tropical storms and hurricanes on submerged bank reefs and coral communities in the northwestern Gulf of Mexico

A. Lugo-Fernández [a,*], M. Gravois [b]

[a] Physical Sciences Unit (MS 5433), Minerals Management Service, 1201 Elmwood Parkway Boulevard, New Orleans, LA 70123-2394, USA
[b] Mapping and Automation Unit (MS 5413), Minerals Management Service, 1201 Elmwood Parkway Boulevard, New Orleans, LA 70123-2394, USA

ARTICLE INFO

Article history:
Received 12 March 2009
Received in revised form
15 January 2010
Accepted 8 March 2010
Available online 1 May 2010

Keywords:
Gulf of Mexico
Submerged coral reefs
Tropical storm climatology
Sediment resuspension
Larvae dispersal
Coral cover

ABSTRACT

A 100-year climatology of tropical storms and hurricanes within a 200-km buffer was developed to study their impacts on coral reefs of the Flower Garden Banks (FGB) and neighboring banks of the northwestern Gulf of Mexico. The FGB are most commonly affected by tropical storms from May through November, peaking in August–September. Storms approach from all directions; however, the majority of them approach from the southeast and southwest, which suggests a correlation with storm origin in the Atlantic and Gulf of Mexico. A storm activity cycle lasting 30–40 years was identified similar to that known in the Atlantic basin, and is similar to the recovery time for impacted reefs. On average there is 52% chance of a storm approaching within 200 km of the FGB every year, but only 17% chance of a direct hit every year. Storm-generated waves 5–25 m in height and periods of 11–15 s induce particle speeds of 1–4 m s^{-1} near these reefs. The wave–current flow is capable of transporting large ($\sim$3 cm) sediment particles, uplifting the near-bottom nepheloid layer to the banks tops, but not enough to break coral skeletons. The resulting storm-driven turbulence induces cooling by heat extraction, mixing, and upwelling, which reduces coral bleaching potential and deepens the mixed layer by about 20 m. Tropical storms also aid larvae dispersal from and onto the FGB. Low storm activity in 1994–2004 contributed to an 18% coral cover increase, but Hurricane Rita in 2005 reduced it by 11% and brought coral cover to nearly pre-1994 levels. These results suggest that the FGB reefs and neighboring reef banks act as coral refugia because of their offshore location and deep position in the water column, which shields them from deleterious effects of all but the strongest hurricanes.

Published by Elsevier Ltd.

1. Introduction

The beauty and apparent tranquility of coral reefs belie the dynamic and complex structure that makes coral reefs one of the most persistent ecosystems on Earth (McClanahan et al., 2002; Lugo et al., 2000). This appearance of tranquility is reinforced by near-uniform and slowly occurring environmental changes surrounding reefs in tropical seas. However, coral reefs in the tropical biotope are exposed to tropical storms and hurricanes, which many believe to be among the primary causes of coral damage, mortality, and reef modification in the western Atlantic province (Longman, 1981; Woodley et al., 1981; Scoffin, 1993; Blanchon et al., 1997; Aronson and Precht, 2001).

Reports of storm and hurricane impacts on coral reefs abound in the literature; if climate change increases their frequency or intensity (Riegel, 2007; Emanuel et al., 2008), we will have more opportunities to better understand the effects of these "disturbances." Indeed, the price of this knowledge will likely be high! Harmelin-Vivien, (1994) reviewed and synthesized many reports of hurricane–coral reef interactions up to 1994; since then, specific examples of hurricane–reef reports include Lugo-Fernández et al. (1994), Van Veghel and Hoetjes (1995), Van Woesik et al. (1995), Precht et al. (2008a), and the reviews and summaries by Gardner et al. (2005) and Riegel (2007), among others.

Impacts of tropical storms and hurricanes on coral reefs are either physical or biological in character. Physical impacts include mechanical damage by waves, currents, and projectiles; damage by sedimentation (burial, abrasion, and exposure); turbidity damage caused by resuspension and runoff; and salinity reduction by rain and river runoff (Harmelin-Vivien, 1994). A positive impact of storms and hurricanes is the creation of new landforms such as cays and boulder ramparts (Hernández-Ávila et al., 1977), submerged bars and sediment aprons (Scoffin, 1993), but when sediment removal and re-deposition destroy these cays this impact is negative (Dollar, 1982). Negative biological impacts include disruption of reef zonation by destruction and damage of coral colonies (Woodley et al., 1981; Dollar, 1982; Grauss et al., 1984; Sorokin, 1995), coral cover reduction (Gardner et al., 2005), and a reduction of algae cover (McClanahan et al., 2002). Positive

* Corresponding author.
E-mail address: alexis.lugo.fernandez@mms.gov (A. Lugo-Fernández).

0278-4343/$ - see front matter Published by Elsevier Ltd.
doi:10.1016/j.csr.2010.03.014

biological effects include mitigation of bleaching by storm-induced cooling (Van Veghel and Hoetjes, 1995; Manzanello et al., 2007), opening of space to growth and recruitment (Rogers, 1993; Treml et al., 1997), and helping coral dispersal by fragmentation and larvae dispersal (Gardner et al., 2005; Lugo-Fernández et al., 2001).

Tropical storm and hurricane impacts on coral reefs are not simple linear processes but are complicated highly nonlinear processes, whose results can be confusing and even surprising (Scoffin, 1993; Harmelin-Vivien, 1994). At a basic level, the observed effects on coral reefs depend on the specific characteristics of storms and hurricanes, reefs, and their interactions. Nine relevant storm aspects that influence impacts to corals are listed below (Treml et al., 1997; Lugo et al., 2000; Bythell et al., 2000):

1. Geographical distribution	4. Size	7. Storm surge
2. Frequency	5. Forward Speed	8. Induced waves and currents
3. Intensity	6. Distance and orientation relative to reef	9. Rain

Ten relevant aspects of coral reefs that help determine storm impacts are listed below (Treml et al., 1997; Lugo et al., 2000; Bythell et al., 2000; Gardner et al., 2005):

1. Reef's geographical location	6. Colony depth
2. Reef morphology;	7. Reef's pre-hurricane health
3. Community structure	8. Reef's position relative to storm track
4. Colony size	9. Skeleton's strength
5. Colony morphology	10. Reef's previous exposure to hurricanes

Other relevant factors for interaction between storms and hurricanes and reefs are the adjacent land geography, the resulting freshwater runoff, and the ensuing turbidity and sediment effects on colonies (Treml et al., 1997). Factors seldom mentioned in the literature of storm–coral reef interaction are the shelf's geography and pre-storm hydrographic conditions, which affect the ocean's response to the storm forcing. Another factor seldom examined is the near reef bottom sediment cover, which can affect corals and optical conditions at the reef (Sosik et al., 2001). All impacts depend on the important probability of storm contact with a reef, which is a function of storm climatology and reef's location.

The fact that present-day Caribbean coral reef communities and hurricanes have co-existed for at least 5000–6000 years when the rate of sea level slowed following the last glacial minimum (Glynn, 1973; Donnelly and Woodruff, 2007) and that coral reefs persist today suggests that coral reefs recover from storm impacts relatively fast over long time scales of geology and ecology. The available information indicates that coral reefs recover, in general, over spans of 10–25 years (Glynn, 1973; Woodley, 1992; Sorokin, 1995; Pandolfi and Jackson, 2007; Gardner et al., 2005; Grauss et al., 1984), but periods as low as 2–8 years and as high as a century are needed for recovery (Harmelin-Vivien, 1994).

This study examines tropical storm and hurricane interactions with submerged coral reefs of the Flower Garden Banks (FGB) in the Louisiana–Texas (LATEX) shelf, northwestern Gulf of Mexico, Fig. 1. The FGB are located at the shelf's edge and far from the nearest shoreline. In addition to these two banks, other topographic banks with coral communities on this shelf are also exposed to tropical storms and hurricanes. In this study we (1) developed a storm and hurricane climatology for the FGB and neighboring banks, (2) employed this climatology to derive estimates of storm and hurricane-induced waves and currents to assess physical damage and sediment resuspension, (3) derived the probability distribution of storm and hurricane–reef interaction, and (4) examined the relationship between storms and coral cover. The effects of storm currents on larvae dispersal and reef connectivity are also discussed. This work differs from previously published reports in several ways: (1) it is not a forensic analysis of a specific event, (2) it consists mainly of applying mathematical relationships and observations to estimate potential physical damage and compares this with available reports, (3) unlike most studied reefs, these are shelf edge reefs far from land, and (4) these reefs are submerged banks rather than the more familiar fringing or barrier reefs close to sea level, on which most of the available storm and hurricane-impact literature has focused.

2. Study area

The FGB in the northwestern Gulf include the East Bank (EFGB; 27°54′N, 93°35′W) and the West Bank (WFGB; 27°52′N, 93°48′W) coral reefs at the edge of the LATEX shelf and ~200 km off the Louisiana coastline (Fig. 1). These banks, ~18 km apart, are two of many topographic prominences distributed over the shelf edge (Gardner et al., 1998). From shelf depths of 100–150 m, they rise to within 18 m of the sea surface. The lower 30–35 m of both banks are generally covered by a nepheloid layer (suspended muddy sediments), which limits coral growth; however, the upper 50 m of these banks are exposed to oceanic conditions that favor reef growth (e.g., Rezak et al., 1985; Deslarzes, 1998).

Shallower areas of the FGB reef contain at least 24 hermatypic coral species (depth range: 15–52 m, reef cover ~2.1 km^2 at the EFGB and 0.6 km^2 at the WFGB; Bright and Pequegnat, 1974; Bright et al., 1984; Rezak et al., 1990; Schmahl et al., 2008). Many coral species on the FGB (including *Madracis decactis*, *Siderastrea* spp., *Stephanocoenia* spp., *Diploria strigosa*, *Montastraea cavernosa*, and *Agaricia* spp.) exist also on neighboring banks (e.g., Sonnier Bank, Stetson Bank, and Bright Bank, Fig. 1), but form less coral cover (scattered, small colonies; Rezak et al., 1985). Since 1990 the broadcast spawnings of seven reef building species, which make up ~82% of the coral cover, have been witnessed at the FGB (Gittings et al., 1992a, 1992b; Hagman et al., 1998; Boland, 1998; Schmahl et al., 2008). Mass spawning at the FGB is synchronous with spawning at other Caribbean reefs, is correlated with lunar phase, and occurs during summer's maximum water temperature (Gittings et al., 1994; Hagman et al., 1998). Mass spawning in the western Atlantic also coincides with the hurricane season (Rogers, 1993; Lugo-Fernández et al., 2001).

Hydrographic conditions and currents around the FGB are reviewed in Lugo-Fernández (1998). Currents near the FGB, strongly influenced by mesoscale deep-water processes, flow mainly west–east with mean speeds of ~0.08 m s^{-1}, but under normal conditions they can reach up to 0.75 m s^{-1} near the surface and decrease to ~0.01 m s^{-1} near the bottom (Nowlin et al., 1998). Because of large distance from the shore, the FGB reefs are generally shielded from the brackish, muddy, and opaque near-shore waters; however, usually in late May–July, parcels of mixed nearshore and offshore waters reach near the FGB (Deslarzes and Lugo-Fernández, 2007). These fresher waters (S~30–32) can bring nearshore pollutants and particles, and increase light attenuation of otherwise clear waters near these reefs. Reports have been made of extreme waves at the FGB occurring mostly during tropical storms and hurricanes in summer and during the passage of cold fronts in winter (McGrail, 1983; Nowlin et al., 1998; Schmahl et al.,

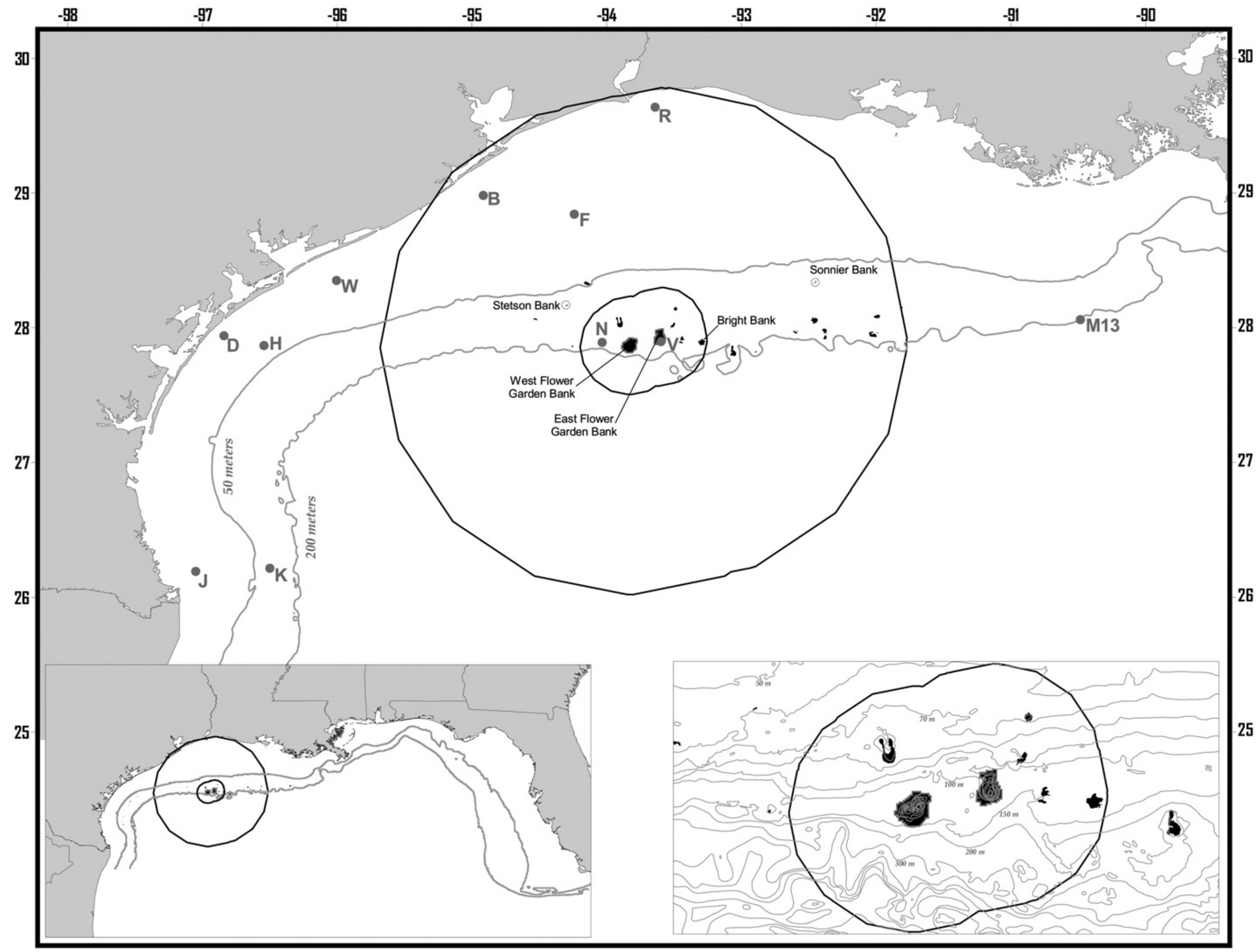

Fig. 1. Map showing location of the Flower Garden Banks reefs and other topographic banks, e.g., Stetson, Bright, and Sonnier Banks within 200-km and 36-km buffer zones. Also shown are buoys and current meter mooring (M13) employed in this study. Right inset shows the FGB with detailed bathymetry and left inset shows the FGB relative to the northern Gulf of Mexico.

2008). These waves are accompanied by oscillatory currents of $\geq 1.4\,m\,s^{-1}$ (Lugo-Fernández, 1998).

3. Methods

Track data of tropical storms and hurricanes were obtained from the National Hurricane Center database titled "Historical North Atlantic Tropical Cyclone Tracks: 1851–2006," available online at http://www.csc.noaa.gov/hurricane_tracks. This database includes data, gathered at 6-h increments, of center locations, and storm and hurricane intensities. Data for each increment include year, month, day, time, storm unique identifier, name, latitude, longitude, wind speed, central pressure, Saffir–Simpson's category, and basin of occurrence. To make the most of the hurricane data, we selected hurricane tracks from 1900 to 2006. This subset also reflects a compromise between the number of data and uncertainty in track information, which is discussed later.

A circular buffer of a 200-km radius was delineated around the banks; all storms whose tracks intersected the buffer were deemed as affecting the FGB and selected for analysis. The reasons for establishing the buffer's radius were: (1) small tropical storms have radii >300 km; (2) there are reports of reef damage by storms and hurricanes that passed 145 km away or greater (Van Veghel and Hoetjes, 1995; Harmelin-Vivien, 1994); (3) Manzanello et al. (2007) found that, when passing at distances of ≤ 400 km from a reef, hurricanes can strongly affect water temperature; (4) Chang and Guo (2007) found tropical hurricane effects up to 300 km from ships and land masses; and (5) 200 km is just above the most frequent radius of tropical storms winds (Dean et al., 2009). We expect our buffer to capture most storms and hurricanes that affected the FGB given that very small storms have radii ≤ 200 km. Since several smaller topographic banks (e.g., Stetson Bank to the northwest of the FGB; (Fig. 1)) that harbor reef communities lay inside the buffer, our analyses and results are relevant for these neighboring banks.

Data about the relevant track increments were analyzed to establish the storm climatology for these banks. Statistical analyses determined the statistical frequency distributions of

1. number of storms per decade,
2. number of Category 3 to 5 hurricanes per decade,
3. number of storms per month,
4. storm's categories, and
5. storm's direction of approach.

The analysis also contributed to estimating contact probabilities and producing a scatter plot of wind speeds around the FGB. A smaller buffer zone of 36 km, Fig. 1, was delineated to estimate the number of direct hits. This buffer size was based on the premise that the strongest hurricanes typically have small eye radii and on previous reports that most intense damages occur within this area (Frank, 1977; Simpson and Riehl, 1981; Treml et al., 1997).

After completing the storm climatology, we examined impacts of hurricane-driven oceanographic processes. Among the most notable hurricane effects are reduction of sea surface temperature, generation of strong inertial motions, large internal and surface waves, and cooling of the surface mixed layer (Zedler et al., 2002). A less known effect is sediment resuspension with concurrent changes of optical attenuation coefficients (Chang et al., 2001; Sosik et al., 2001). A hindcast of hurricane surface waves was conducted following the *Shore Protection Manual* procedures (USCOE, 1984). The hindcast was based on representative or typical hurricane values of central pressure, radius of maximum winds assumed to equal the eye radius, and translational speed. Translational or forward speed was estimated by dividing the buffer diameter (=400 km) by 18 h, which is the transit time of storms crossing the buffer from individual tracks. Additionally, a hindcast was conducted of a hurricane that hit the FGB on September 23, 2005 (Hurricane Rita). Wave heights of tropical storms were estimated at (1) a distance of 198 km from the storm's center, which is the distance at which their maximum wind occurs (Simpson and Riehl, 1981) and (2) the distance at which hurricane winds decrease to tropical storm-wind strength generally. These estimates of wave height and period were used with linear wave theory to calculate orbital speed, acceleration, and wave-induced forces on the *M. cavernosa* and *D. strigosa* coral species. These species were selected because they are the most dominant corals and account for 37% of coral cover at the FGB reefs (Gittings, 1998). The FGB lacked branching corals, such as *Acropora palmata*, until two small colonies were discovered very recently (Aronson et al., 2005). The hydroid *Millepora alcicorni* with a cylindrical shape occurs within the FGB. Additionally, orbital speed was utilized to estimate sediment resuspension. A wave–current interaction model (Mei, 1983) was employed to calculate lifting of particles from the near-bottom nepheloid layer surrounding the banks at depths of ~100 m. Coral reefs of the FGB are at water depths of ~18 m or a height of ~82 m above the bottom. We also examined the intense hurricane-driven mixing and entrainment of deep water, which destroys the strong summer stratification observed at the FGB. Hurricane effects on larval dispersal were discussed using published observed surface drifter information during storms or hurricanes. Finally, an analysis of storm effects on coral cover change at the FGB was conducted.

4. Results

4.1. Storm climatology

Seventy-nine (79) storms interacted with the FGB coral reefs between 1900 and 2006 according to the track data (Fig. 2). Technologies used to observe tropical storms underwent two major changes—the use of aircraft in the mid-1940s and the advent of satellites in the late 1960s (Chang and Guo, 2007; Landsea, 2007). Because of these changes the observations after 1950 are widely accepted as the most reliable data on storm track. Based on this information the track data were divided into 1900–1949 and 1950–2006 as an attempt to separate any observational bias in the number of storms. We also wanted to capture the two most active storm periods in the Atlantic basin, 1926–1955 and 1995–2005 (Chang and Guo, 2007; Landsea, 2007). The uncertainty is larger in the early 1900s, amounting up to almost 10 storms per decade for the 1920s and 1930s (Chang and Guo, 2007); however, the bias decreases rapidly from 1940 to 1950 since flights to detect storms were initiated. Another factor reducing the observational bias in our study is that west of 50°W longitude, where the FGB are located, the storm count is accurate because storms make landfalls (Chang and Guo, 2007; Landsea, 2007). The number of storms affecting the FGB in 1900–1949 is 40 but could be higher if corrected for bias, and 39 in 1950–2006. Thus, it seems that, for this locality, the observational bias seems small. The average number of storms affecting the FGB is 3 every 4 years, but in a given year this number could be different because of the 30–40 year cycle in Fig. 3. In the early 1900s the number of storms was high (8), decreased to a minimum in the 1920s, increased to 14 in the 1940s, decreased to 4 in the 1960s, rose to 6 in the 1980s, declined in the 1990s, and ended on a high of 5 in the early 2000s. This cycle nearly matches the 30–40 year variation of storms in the Atlantic basin (see NOAA figure at 〈http://www.nhc.noaa.gov/pastprofile.shtml〉; Goldenberg et al., 2001). It is noteworthy that the number of Category 3–5 hurricanes in Fig. 3 that affect the FGB is higher in the 1900–1950 period and decreases in the 1950–2006 period. This result is contrary to that observed for the Atlantic basin, which had less strong hurricanes in the 1900–1950 and higher in the 1950–2006 period, probably reflecting the increased observational database and climatic forcing (Goldenberg et al., 2001).

The monthly distribution of storms at the FGB, Fig. 4, shows that September is the month of highest storm activity with 25, followed by August with 23. July and October have similar levels of activity with about 10 storms. May and November are the months of lowest storm activity, with one occurrence each. This distribution agrees with the distribution of storms and hurricanes in the Atlantic basin (see NOAA figure at http://www.nhc.noaa.gov/pastprofile.shtml). The fact that storm activity is high in midsummer could be beneficial as it raises the likelihood of lowering summer's high temperatures of ~30 °C (Lugo-Fernández, 1998) by mixing and upwelling. This cooling reduces the potential for coral bleaching (Manzanello et al., 2007). Furthermore, storm peak activity coincides with FGB mass spawning and may raise larval dispersal potential (Lugo-Fernández et al., 2001).

Fig. 5 shows the frequency distribution of storm type. The most frequent type is the tropical storm with winds of $\leq 17\ \mathrm{m\,s^{-1}}$ ($62\ \mathrm{km\,h^{-1}}$) and significant wave heights of 4–8 m, followed by Category 1 hurricanes with winds of $33–42\ \mathrm{m\,s^{-1}}$ ($119–153\ \mathrm{km\,h^{-1}}$) and wave heights of 8–10 m. The most damaging storms impacting the FGB are the Category 4 and 5 hurricanes with winds of $>58\ \mathrm{m\,s^{-1}}$ ($210\ \mathrm{km\,h^{-1}}$) and wave heights of 12–15 m. Hurricane Rita in 2005 was Category 3/4 when it impacted the FGB. During the study period, only one Category 5 hurricane, Hurricane Carla in 1961, affected the FGB for only 6 out of 18 h of interaction.

Fig. 6 shows the distribution of storm approach to the FGB. Most storms affecting the FGB approach from the southeast (SE) direction. Storm approaches from the northeast and southwest have nearly equal frequencies at 10–20%. Surprisingly, this figure reveals that storms approaching from the northwest do occur. Storms approaching from the northeast and northwest indicate storms that reach the FGB from land, which most likely means that these storms curled back to sea! Storms from the southwest are indicative of storms that form over the southwestern gulf and/or Mexican waters.

Storm tracks reveal 20 direct hits to the FGB from 1900 to 2006. A direct hit means that a storm approached the FGB within 36 km, which is a typical or representative eye radius of a very

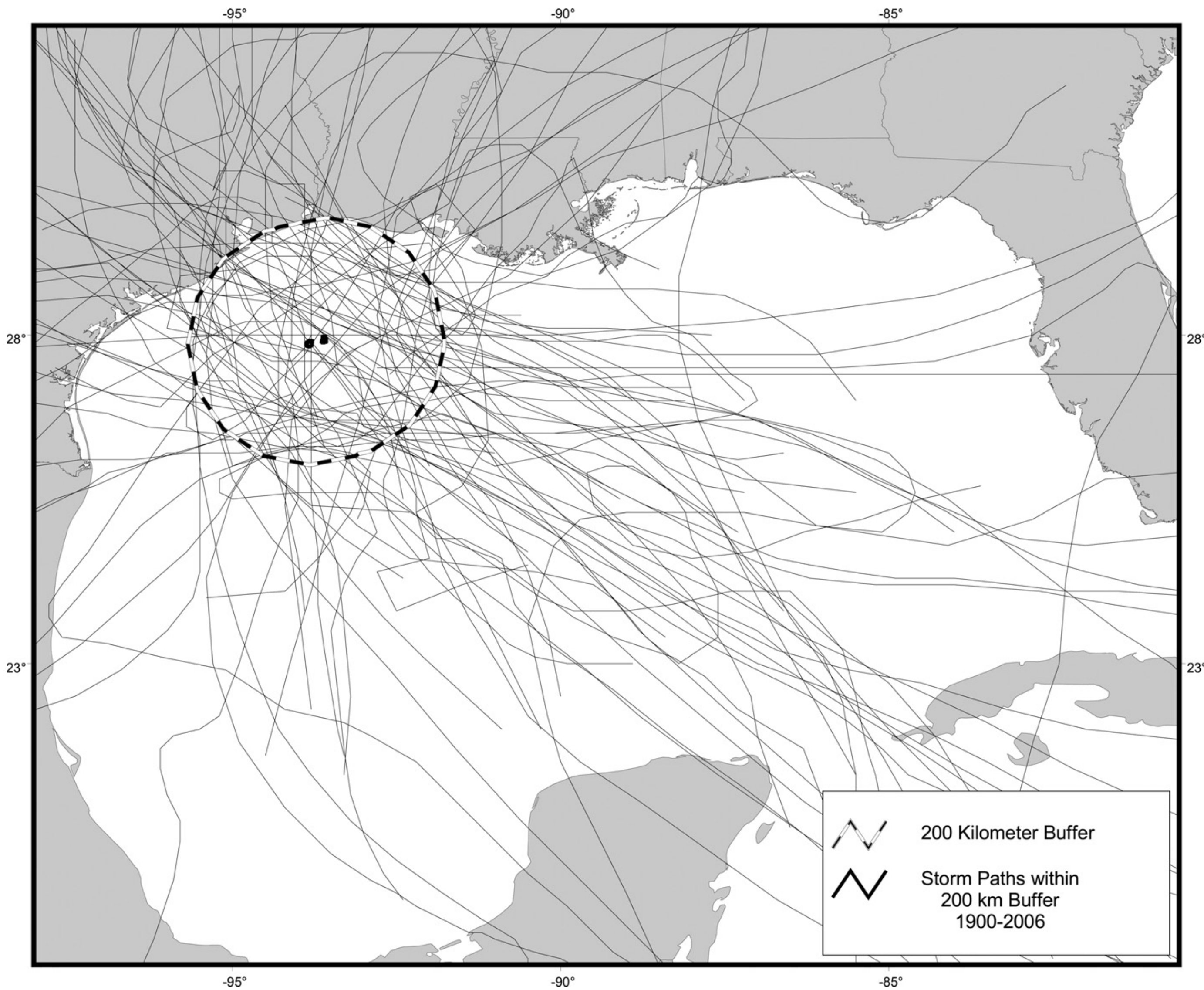

Fig. 2. Map showing tracks of the 79 storms that came within the 200-km buffer zone around the reefs of the Flower Garden Banks from 1900 to 2006.

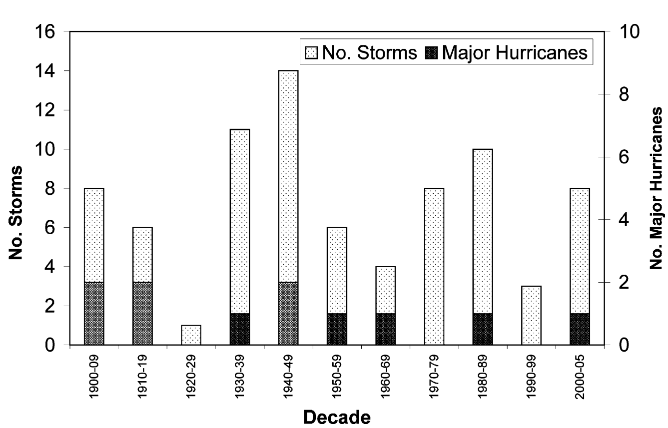

Fig. 3. Bar chart showing decadal number of tropical storms and major hurricanes contacting the FGB reefs from 1900 to 2006. Notice the long-term (~40 year) cycle in the number of storms similar to that observed in the Atlantic basin.

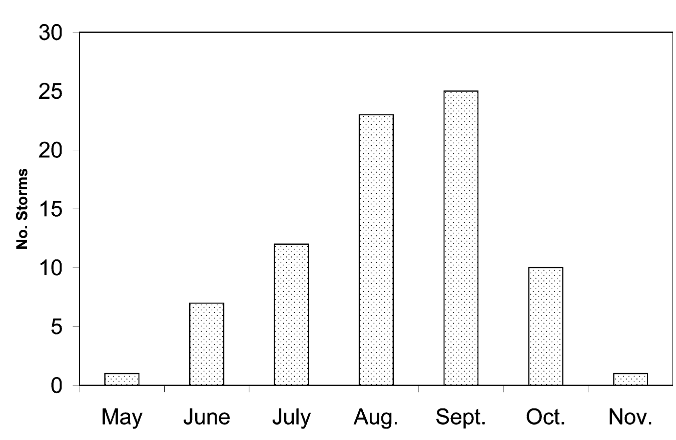

Fig. 4. Monthly distribution of tropical storms and hurricanes contacting the FGB from 1900 to 2006.

strong hurricane. These direct hits take place at an average rate of one per 5–6 years, which, as expected, is less frequent than contacts with the FGB. The 20 direct hits are distributed nearly evenly over time with 9 between 1900 and 1950, and 11 between 1950 and 2006, which is similar to the number of storms affecting the FGB. However, the storm type is not evenly distributed;

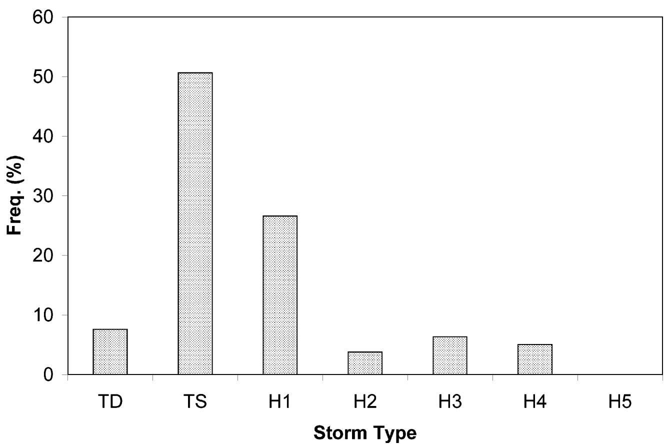

Fig. 5. Distribution of storm category contacting the FGB from 1900 to 2006. Note that no Category 5 hurricane contacted the FGB from 1900 to 2006.

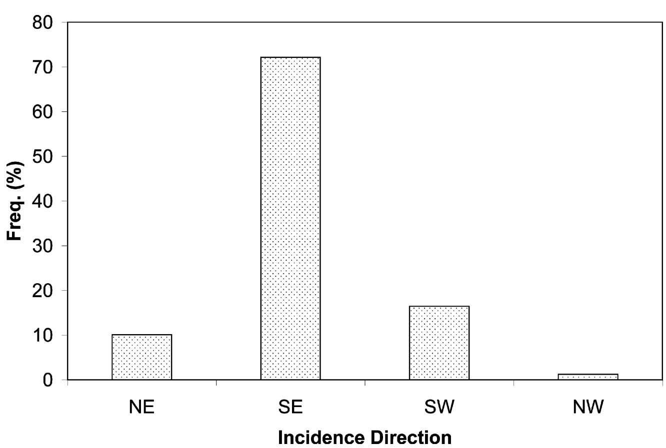

Fig. 6. Distribution showing the direction of approach for all storms contacting the FGB from 1900 to 2006. The predominant direction of approach is from the SE and surprisingly storms have approached the FGB from land.

there were 6 strong-hurricane direct hits in 1900–1950 vs. 3 in 1950–2006. This result reflects the fact that the number of strong hurricanes affecting the FGB is higher between 1900 and 1950. A scatter plot of wind speed derived from the track data is shown in Fig. 7. As expected, this figure shows that tropical storm strength winds are the most frequent. This figure also reveals that both banks have been impacted by Category 4 hurricane winds, while winds of Category 3 and 1 hurricanes have occurred very close to the FGB. Fig. 7 also shows the single occurrence of Category-5 winds inside the buffer zone. Category 5 winds persisted near the FGB for 6 h in 1961.

Finally, we estimated the frequency distribution of storms contacting the FGB reefs. It is important to reiterate that a contact is not a direct hit, but a measure that a storm or hurricane came within the 200-km buffer around the FGB. The results are shown in Fig. 8. As expected, the figure shows that as the number of contacts per year increases, the frequency decreases. No-contact in a year has a frequency of 48%, and for one or more contacts in a year the frequency is 52%. Thus, it seems there is a 52% chance of the FGB reefs being contacted or a storm or hurricane coming within a 200-km radius each year. Again, this is not the likelihood of a direct hit! In greater detail, there is 29% chance of one contact per year, 22% chance of two contacts per year, and 0.9% chance of three contacts in a year. The number of storm contacts with the FGB is similar to counting accidents at an intersection, which is described by a Poisson distribution. The Poisson distribution requires only one parameter to estimate probabilities, the average number of storms contacting the FGB per year, which is 3 storms per 4 years or 0.745 storm per year. The estimated probabilities using this rate are also shown in Fig. 8. The overall conclusion of a 48% chance of no-contact and 52% chance of one or more contacts is corroborated. However, the chance of one contact per year is slightly overestimated (35% vs. 29% observed), while for two contacts the estimate is lower (13% vs. 22% observed), and for 3 contacts, the estimate is higher (3% vs. 0.9% observed). The main result is that the FGB have a 52% chance of interacting with a storm every year. How well does the Poisson distribution describe the observations of storm contacts with the FGB? A chi-square goodness of fit test reveals that the Poisson distribution performs well at the 99% confidence level. However, there is a caveat; the number of bins with the minimum number of observations required was only 3, so the power of the test could be compromised because of the limited number of observations.

4.2. Oceanographic processes

In deep waters near the FGB, high wind speeds during storms and hurricanes generate strong currents ($\sim$1.0 m s^{-1}) and large waves ($H \geq 5$ m), which drive high levels of turbulence, upwelling, and mixing of water, mixed layer cooling, resuspension of sediments, and large forces on the flora and fauna of these coral reefs. These processes affect shallow-water reefs by causing destruction and mortality of corals through uplifting and transport (e.g., Glynn et al., 1964; Graus et al., 1984; Harmelin-Vivien and Laboute, 1986), lowering salinity (e.g., Glynn, 1973), and morphological changes and sediment movements (e.g., Stoddart, 1962, 1969; Hernández-Ávila et al., 1977; Lugo-Fernández et al., 1994).

To predict storm-induced waves requires the Coriolis parameter, which at the FGB's latitude (27.7°N) is 0.244 h^{-1}. The required radii of maximum winds for the storm types considered here are 54 km for a Category 1 hurricane, 45 km for a Category 2, and 36 km for a Category 3–4 hurricane derived from a wind model in Simpson and Riehl (1981). As expected, radii variations from these "typical" values do occur. Table 1 shows the wave hindcast with parameters typical of the hurricanes contacting the FGB reefs. Significant waves (H_s) near the center of the hurricanes ranged from 8 to 11 m, maximum waves (H_{max}) ranged from 15 to 20 m, and wave periods (T) ranged from 11 to 13 s. Hindcast significant wave heights during or at tropical storm winds (H_{ts}) ranged from 4.7 to 5 m. The hindcast tropical storm wave heights compared very well with wave height observations at the FGB of 5 m and periods of 10 s (McGrail, 1983). Hindcast hurricane waves compare well with the 9-m and 16-s periods observed on the northern shelf of the Gulf of Mexico about 350 km east of the FGB during Hurricane Andrew (DiMarco et al., 2001). A further comparison and validation of hindcast waves can be made by noting that the significant wave height under Hurricane Ivan was $\sim$17 m (Wang et al., 2005) and $\sim$12 m under Hurricane Lili as measured by NDBC buoys. Finally, note that the 100-year wave height (wave height with a 100-year return period) for the gulf is $\sim$10 m (Panchang and Li, 2006), which is exceeded by waves during Category 3–5 hurricanes.

Hurricane Rita (September 23, 2005) was one of the strongest hurricanes since observations started in the Gulf of Mexico, and crossed near the FGB as a Category 3 hurricane. The hindcast for Hurricane Rita indicates significant waves of about 14 m, maximum wave height $\sim$26 m, and period of 14 s. The estimated tropical storm wave height is $\sim$8 m. For comparison, the reported significant wave height at NDBC Buoy No. 42019 ($\sim$152 km west of the FGB) was 4.5 m, and our estimate for that side and distance

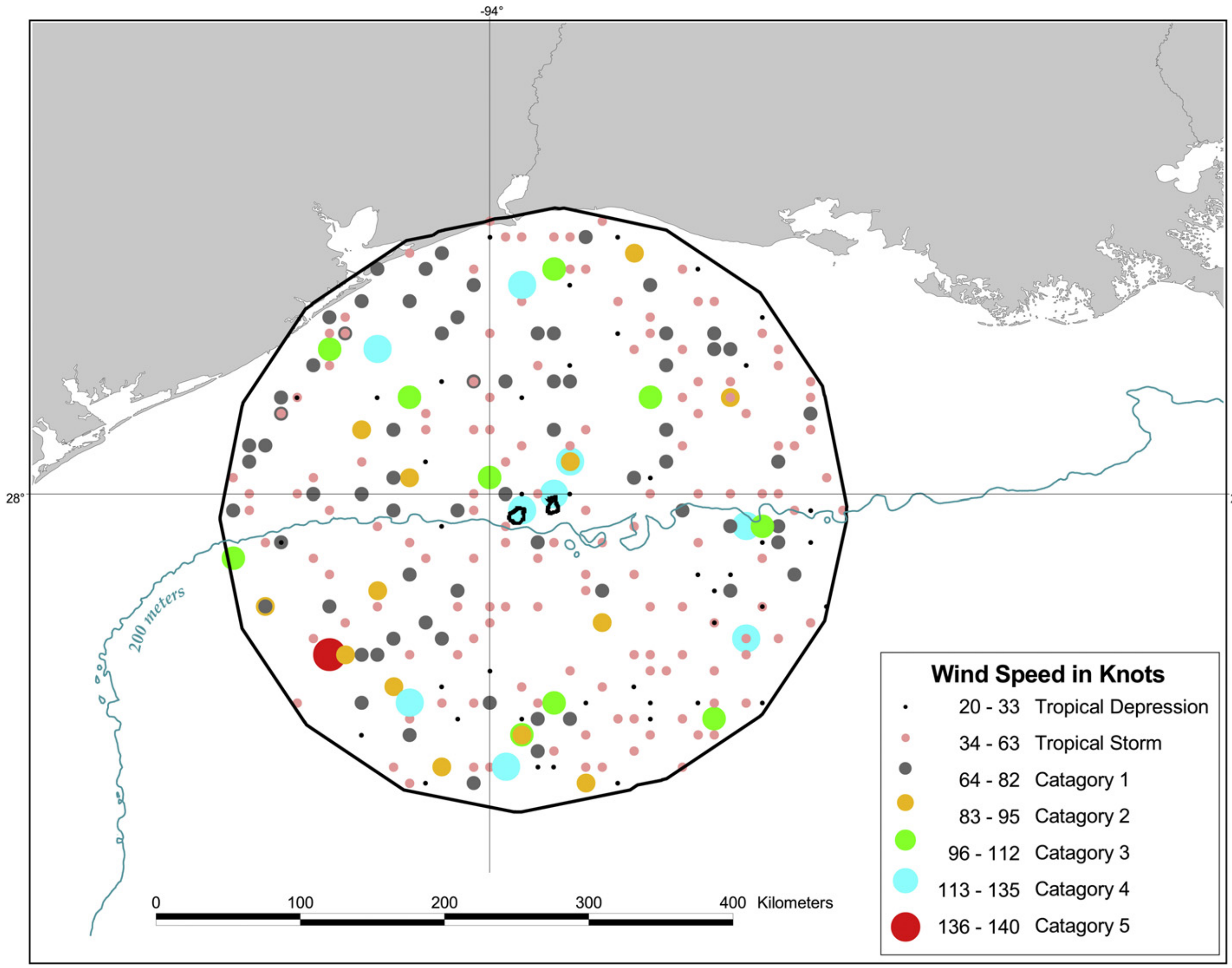

Fig. 7. Distribution of wind speed affecting the FGB reefs. Notice that the FGB have experienced Category 5 winds even when no Category 5 hurricane has affected the FGB reefs.

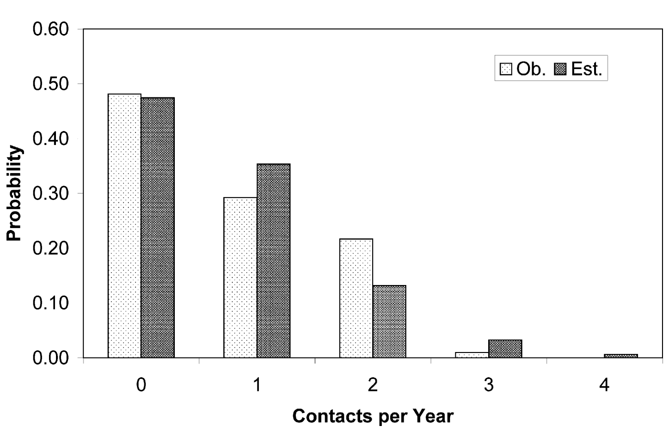

Fig. 8. Observed frequency of storms contacting (not direct hits) the FGB annually. Note that there is about 50% chance every year of a tropical storm contacting the FGB.

Table 1
Hindcast of significant wave height (H_s), maximum wave height (H_{max}), tropical storm wave height (H_{ts}), and wave period (T) of typical Category 1–3 hurricanes and Rita in 2005 (Category 3) at the FGB as a function of translation speed (V).

V	6 (m s^{-1})				10 (m s^{-1})			
	H_s (m)	H_{max} (m)	T (s)	H_{ts} (m)	H_s (m)	H_{max} (m)	T (s)	H_{ts} (m)
H-1	8.4	15.4	11.2	5.0	9.7	17.6	12.0	5.8
H-2	9.1	16.4	11.7	5.0	10.4	18.6	12.5	5.7
H-3	10.2	17.9	12.3	4.7	11.5	20.1	13.1	5.3
Rita	12.9	23.2	13.9	7.7	14.6	26.1	14.8	8.7

from the hurricane center is less than 5.8 m. At Buoy 42035 (~158 km northwest of the FGB), the observed wave height was 6.1 m, which matches our 6.1 m estimate. The latter buoy is closer to Rita's track, which could explain some of the differences between estimated and observed wave heights. Thus, our hurricane wave hindcast at the FGB reefs seems reasonable.

Possible wave forces on coral and hydroid colonies of the FGB reefs were estimated using Morison's equation

$$F=\frac{1}{2}\rho u^2 C_d S_p+\rho V C_m \frac{\partial u}{\partial t},$$

where ρ is the fluid density (=1025 kg m^{-3}), u the wave particle speed from linear theory, du/dt the wave-induced acceleration from linear wave theory, S_p the body area presented to the flow,

V the body's volume, C_d the drag coefficient, and C_m the inertia coefficient. For this work we calculated forces for *Montastrea* and *Diploria* corals in the WFGB because these are the most common coral species on these reefs. We approximated these colonies as hemispheres whose $C_d = 0.32$ and $C_m \approx 2C_d = 0.64$ (Denny, 1988). Since the WFGB has nearly vertical sides, we estimated reflection and transmission of waves from this bank, but these processes were ignored because the estimated transmissions coefficients (see Mei, 1983, p. 132 for formulas) are high (0.86 for $T = 8$ s to 0.96 for $T = 14$ s). The wave forces and particle velocities estimated over a wave cycle near the floor of the reef are shown in Fig. 9. The wave forces range from 150 N for $T = 11$ s and $H = 5$ m to 1500 N for $T = 14$ s and $H = 15$ m. Two aspects of Fig. 9 are worthy of comment; first, notice how the total wave force changes in shape and symmetry as the wave height and periods increase, i.e., as waves get higher and longer the total force tends to emulate drag forces. This change is caused by the diminishing role of the inertia force when compared with the drag force at higher wave heights and periods, a result that agrees with Denny (1988) and Madin (2005). The second aspect is that both drag and total force tend to have a net or residual effect in the direction of wave travel, i.e., positive, thus yielding a net force in the direction of wave travel.

Denny (1988) defines a wave exposure index as

$$\chi = \frac{F_{max}}{\sigma_b S_p},$$

where F_{max} is the maximum wave force, σ_b the breaking stress ($= 1.8 \times 10^7$ N m^{-2}, Denny, 1988), and S_p the sectional area ($= \pi r^2$). If $\chi < 1$ waves do not cause structural damage and if $\chi \sim 1$ waves cause structural damage or breakage. Note that this index incorporates the geometrical aspect of corals through the force computation and applies to all shapes. Using the force estimates in Fig. 9 with $r \geq 0.5$ m, $\chi \leq 10^{-4}$, which indicates that waves are not structurally damaging these corals; $\chi = 1$ when $r = 5$ mm, which means that for larger coral colonies, very little structural damage will occur. Evidence from the FGB during Hurricane Rita suggests that corals of these reefs were largely unaffected directly by hurricane waves and that most damage was from flying debris (Precht et al., 2008a). Next, we examined the wave effects on *M. alcicornis*, a hydroid species present at the FGB and neighboring banks, which grows as a small cylinder. The analysis employed breaking energy (BE) by assuming that these hydroids behave as cantilevers. The idea is that the cantilever maximum displacement occurs at the tip and work is done during this displacement. The tip's displacement equals $y = fL^4/8EI$ (Denny, 1988), where f is the uniform force per length ($= F/L$), E the Young modulus ($= 6 \times 10^{10}$ N m^{-2}; Denny (1988)), $I = \pi r^4/4$, where r is the cylinder radius ($= 5$ mm), and L the cylinder height ($= 0.1$ m). The work done during displacement equals $F{*}y$, and BE can be estimated by dividing the work by the cylinder's volume. Substituting these relationships, BE equals

$$BE = \frac{F^2 L^2}{8EI\pi r^2}.$$

Employing our force calculations, we estimate that for a force of 150 N, BE $= 1.6 \times 10^4$ J m^{-3}, which nearly equals the breaking energy of calcium carbonate ($\sim 0.6 \times 10^4$ J m^{-3}), and breaking is unlikely to occur. For a force of 1500 N, BE $= 1.6 \times 10^6$ J m^{-3}, which exceeds the hydroid's BE value, suggesting that *M. alcicornis* could suffer damage or break under such hurricane conditions. Indeed, during Hurricane Rita, breakage of *M. alcicornis* was observed at the FGB (K. Deslarzes, personal communication). The results found here that no structural damage of massive colonies occur but that hydroids suffered damage, especially at the tips, are consistent with observations

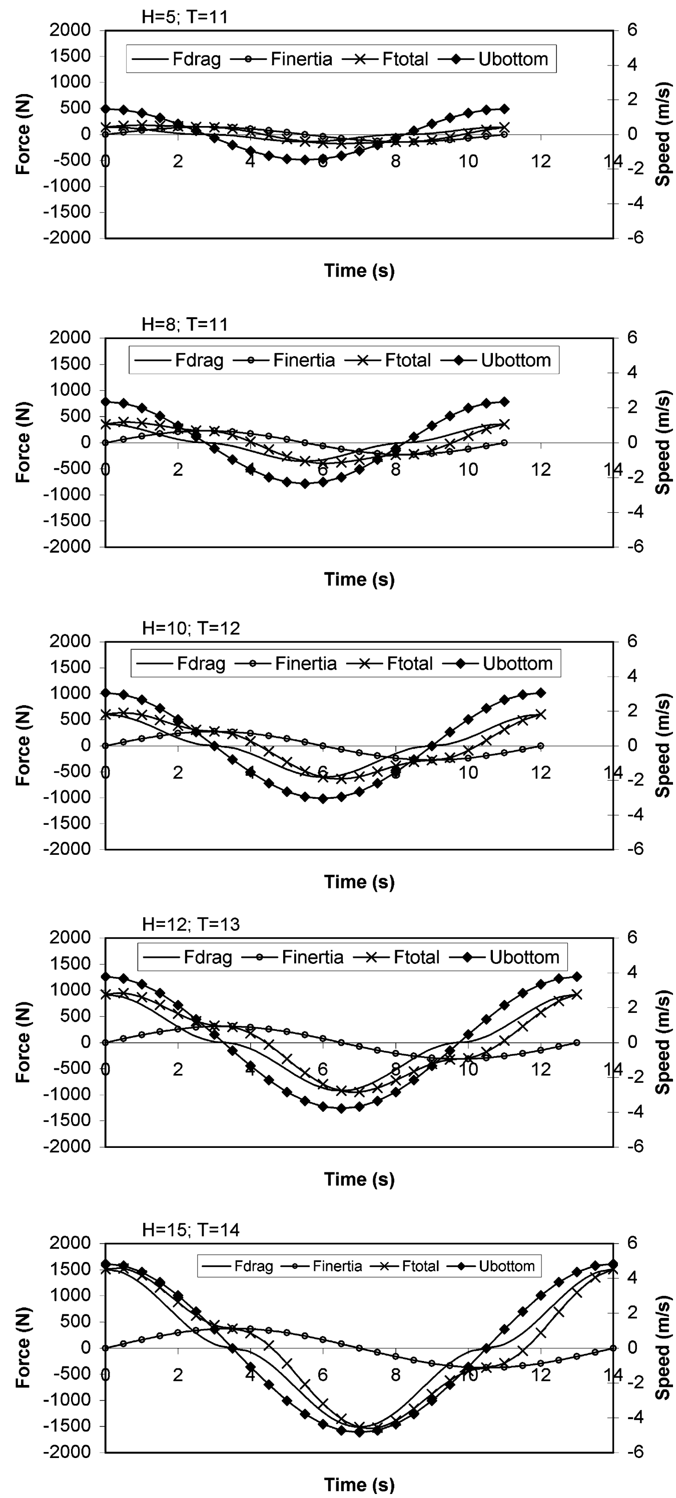

Fig. 9. Particle velocities and wave forces over a wave cycle near the floor of the FGB reefs. Linear wave theory was employed for these calculations.

and theoretical analysis (Precht et al., 2008a; Madin, 2005). Madin (2005) found that most damages by hydrodynamic forces consist of dislodging colonies and hydrodynamic pruning rather than breakage. Pruning is the removal of tips.

Estimated particle velocities (1.5–5 m s^{-1}) near the reef floor under hurricane waves suggest that quartz sediment particles as large as 3 cm would be resuspended and transported. The prevailing strong currents > 0.6 m s^{-1} (Precht et al., 2008a) would transport particles that act as projectiles or abrasive agents.

Large amounts of reef sediment were removed during Rita (Precht et al., 2008a). Because the FGB are raised topographic banks, it is likely that some of these sediments would be transported downslope, thus providing a mechanism for sediment removal from the reefs. Recent analysis of sediments at the base of the banks ranged in calcium carbonate composition from 60% to 100% (Scanlon et al., 2005), confirming our inference that sediment is being lost from these cap reefs. Our results suggest that most sediment losses occur during high energy events. Available photos show that some coral heads were impacted by large objects, which left scars and depressions and killed the coral (Precht et al., 2008a). This type of damage could occur by the movement of falling debris and particles carried by strong currents and oscillatory wave-induced motions, acting as abrasive agents.

4.3. Water and sediment mixing

The large hurricane waves and strong currents interact with the banks' topography, and the ensuing turbulence capable of inducing large mixing is examined below.

Within the surface mixed layer near the FGB the temperature is nearly uniform at 28–30 °C during summer. It is well known that hurricanes leave behind a wake of cooler waters because of heat extraction and wind-induced upwelling (Zedler et al., 2002). If the hurricane is a fast one, it also leaves a trail of near inertial oscillations (e.g., Williams et al., 2001). Cooling was observed at the FGB during Hurricane Rita when the sea-surface temperature decreased by 2–4 °C as shown by satellite images of SST (NOAA Coastwatch Program), and ~2 °C at 18 m over the coral reefs (Precht et al., 2008a). These temperature reductions compare well with temperature drops of ~3–4 °C at the surface and mixed layer after hurricanes in the Gulf and elsewhere (Shay and Elsberry, 1987; Breaker et al., 1994; Chang et al., 2001; Zedler et al., 2002) but are somewhat small compared to ~6 °C cooling at 14 m (current meter mooring 13 in 200 m, see Fig. 1 for location) during Hurricane Andrew in 1992 (Nowlin et al., 1998). The temperature drop at the FGB was short lived, ~1 day, which is much shorter than the ~6 days observed at mooring 13 (Nowlin et al., 1998) and during other hurricanes, which lasted 3–6 days (Williams et al., 2001; Chang et al., 2001; Zedler et al., 2002). The climatology revealed that most tropical storms and hurricanes affect the FGB during August and September, the warmest months with water temperature close to 30 °C (e.g., Lugo-Fernández, 1998). The observed hurricane-induced cooling would lower the water temperature to 24–28 °C, which is below the accepted threshold for bleaching at the FGB (Gittings et al., 1992b), and should result in a reprieve to the FGB corals. Of course, it seems that this reprieve would be ecologically significant only if it lasts several days.

At depths near 100 m, the temperature record at mooring 13 displays oscillations with amplitudes of 4–5 °C and periods of over 24 h, which decreased to near 1 °C by the sixth day. The observed oscillations appear to be inertial, which at this location should have periods of ~25 h. Inertial oscillations are a common ocean response to hurricanes (Shay and Elsberry, 1987) and have been observed at the FGB in connection with other hurricanes by McGrail (1983). These oscillations can have current amplitudes of 0.2–0.3 m s^{-1} over the shelf, but reach >0.6 m s^{-1} at the shelf edge (Chen et al., 1996; Nowlin et al., 1998). The near-surface currents from buoys at the FGB, Fig. 1 (see http://tabs.gerg.tamu.edu/Tglo/) indeed display oscillations with periods of 19–23 h, which could be interpreted as near inertial currents. Maximum observed speeds were 0.3–0.7 m s^{-1}. Because of their oscillatory nature, inertial currents should not induce much water transport, but they could induce stirring. However, interactions with the banks could give rise to nonlinearities with net water transports. The observation of temperature fluctuations at mooring 13 implies that hurricane effects penetrate the water column to a depth of at least 100 m, which at the FGB represents the base of these banks. To further examine the depth of hurricane wind influence, we estimated the Ekman depth (D_E), which was calculated by two methods. First we estimated D_E from its definition $\left(D_E = \sqrt{2\pi A_z/f}\right)$, where A_z is the eddy viscosity (assumed = 0.1 m^{2}s^{-1}, its maximum value over stormy seas; Pond and Pickard, 1983) and f the Coriolis parameter estimated earlier. The D_E estimated this way is 171 m. The second method to calculate D_E follows Pond and Pickard (1983), assuming that the surface velocity is 3% of the wind speed, a commonly accepted estimate. The surface drag coefficient during hurricane conditions estimated from Jarosz et al. (2007) is 1.5×10^{-3} and D_E = 186 m. Both estimates indicate that hurricane effects penetrate to the base of the FGB as the temperature fluctuations show. To explore the accuracy of our methodology, we calculated D_E for non-hurricane conditions using the same formulas but with coefficients representative of calm weather, i.e., A_z = 0.001 m^{2}s^{-1} and a drag coefficient = 1.2×10^{-3} (Pond and Pickard, 1983). The estimated D_E is 17 and 26 m, respectively, which agrees reasonably well with the observed summer mixed layer depth of about 30 m at the FGB. Thus, our result that hurricane effects reach to the base of these banks is robust.

The FGB coral reefs are immersed year-round in the surface mixed layer or layer of wind influence. The mixed layer at the FGB varies seasonally from 70 m in January to 20 m by April (McGrail, 1983). The August–September mixed layer depth of ~30 m at the FGB marks the start of the mixed layer's deepening, which also coincides with the end of the warm period at the FGB, see Fig. 2 in Lugo-Fernández (1998). We lack the measurements needed to determine the deepening of the mixed layer during hurricanes. However, we can make a zero-order estimate using historical information and available measurements during Rita. We constructed a temperature–salinity diagram from data collected at the EFGB at ~20 m during September 20–25, 2005. The diagram shows that temperature ranged from 27 to over 29 °C while salinity remained nearly steady at 36. Only at noon on September 23 did salinity fall to 20–24 for a brief time. Using these data, we estimated the water density or σ_t as ~25.5 kg m^{-3} during the cooler temperatures of 27 °C, as ~25.3 kg m^{-3} during temperatures of 28 °C, and ~25.2 kgm^{-3} during the warmest temperatures of 29 °C. The next step was to employ Fig. 2.26 from McGrail (1983), which shows the seasonal cycle of density and mixed layer depth at the FGB. This diagram essentially represents a solution of the equations needed to estimate the mixed layer depth as a function of time, wind speed, and heat during a seasonal cycle. As such, we employed it to provide a zero-order estimate of mixed layer depth during Rita at the FGB. Essentially, this amounts to assuming that the processes operating on the seasonal cycle are active during a hurricane when it comes to deepening the mixed layer. This is a reasonable hypothesis, given that wind mixing and heat losses are the main agents for seasonal and hurricane deepening of the mixed layer. We did the estimation by looking at the σ_t value that was observed at the reef and then reading the mixed layer depth corresponding to this density. The estimated mixed layer depths are about 58 m for the coolest period and 50–55 m for intermediate and warmer periods. These values agree with observations of mixed layer's depth in the northeastern gulf by Shay and Elsberry (1987). The mixed layer's deepening represents 20–28 m depth increases, and agrees reasonably well with other hurricanes affecting areas of similar depth (Williams et al., 2001). Again, while these are zero-order estimates, they seem reasonable in light of available observations.

Since we have established that hurricane effects penetrate down to the base of the banks or depths of 150–180 m, we should examine the mixing induced by hurricane currents and waves of the nepheloid layer surrounding the FGB at depths of 100 m. This nepheloid layer has a thickness between 20 and 30 m, is present year round (McGrail, 1983), and is composed of terrigenous clastic minerals (Rezak et al., 1983). The vertical concentration of resuspended nepheloid material for a unidirectional, steady, and turbulent flow is

$$\frac{C}{C_a} = \exp\left[\frac{-w_s}{\kappa u_*}(z-a)\right],$$

where C/C_a is a ratio of sediment concentrations; C is the sediment concentration at depth z above the neheploid layer, C_a the sediment concentration at the top of the nepheloid layer (depth$=a$), and w_s the sediment particle settling velocity:

$$w_s = \frac{2gr^2}{9\mu}(\rho_s-\rho),$$

where ρ_s is the sediment density ($=1760$ kg m^{-3}), ρ ($=1025$ kg m^{-3}) the seawater density, g the gravitational acceleration ($=9.8$ m s^{-2}), μ the water viscosity ($=1.14\times10^{-3}$ kg m^{-1} s^{-1}), and r the radius of sediment particles. The settling velocity equation is valid for small particles ($r<0.1$ mm) only. The frictional velocity $u_*=\sqrt{\tau_b/\rho}$, where τ_b is the bottom shear stress and κ is von Karman's constant ($=0.4$); τ_b was calculated using the wave–current interaction model (Mei, 1983, p. 481). Since τ_b depends on the magnitude and angle between currents and waves, we examined two representative cases. In the first case the waves and currents are perpendicular, i.e., the waves are traveling northward and the current is eastward at 0.2 m s^{-1}. In the second case the waves are still northward bound but the currents are directed southwestward at a speed of 0.6 m s^{-1}. This latter case is similar to that observed at the FGB during Hurricane Rita (Precht et al., 2008a). This model requires an effective bottom friction coefficient (f_e), which is determined as in Mei (1983, p. 480). To calculate f_e, we assumed the bottom friction coefficient as 0.006 and the wave friction coefficient (f_w) is from Fig. 7.1 in Mei (1983, p. 415). The bottom roughness needed to estimate f_w was set at 0.001 m, which represents smooth silt/clay sediments near the base of the FGB (Scanlon et al., 2005). The model was evaluated using wave heights of 5–12 m and periods of 10–13 s. These wave conditions nearly cover the entire range in Table 1. Additionally, the thickness of the nepheloid layer was set at 10, 20, and 30 m. The results for case one are shown in Fig. 10 and those for case two in Fig. 11. We must stress that these results are valid for vertically homogenous waters only, which the hurricane mixing tends to establish based on the estimated Ekman's and mixed layer depths. Under low current speeds and small wave heights and periods, i.e., $H\leq7$ m and $T\leq12$ s, Fig. 10 shows very little sediment mixed upward, as shown by concentrations $\leq50\%$ at the FGB tops. When $H\geq7$ and $T=13$ s, the sediment is mixed upward effectively as shown by concentrations of 60–80% at the FGB tops. Under high speed currents, Fig. 11 shows that sediments are effectively mixed upward as shown by concentrations of 60–80% at the FGB tops for nearly all waves and periods examined. Only when $H=5$ m and $T=10$ s do concentrations stay near 40% at the FGB tops. Thus, it seems reasonable to expect

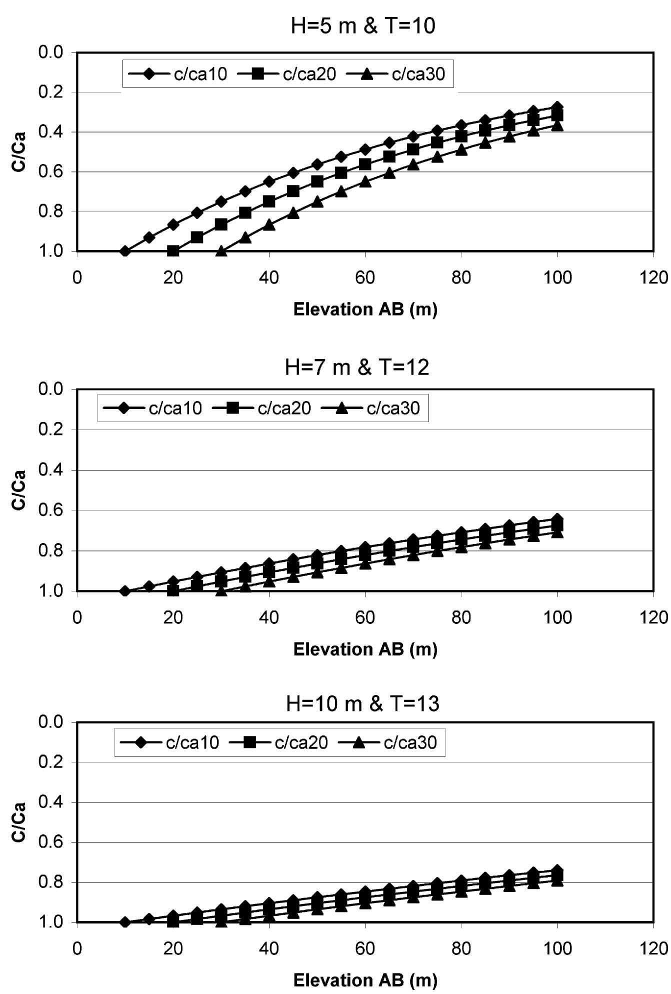

Fig. 10. Vertical concentration of nepheloid material (C/C_a) as a function of wave height and period during tropical storms and hurricanes and low current speeds.

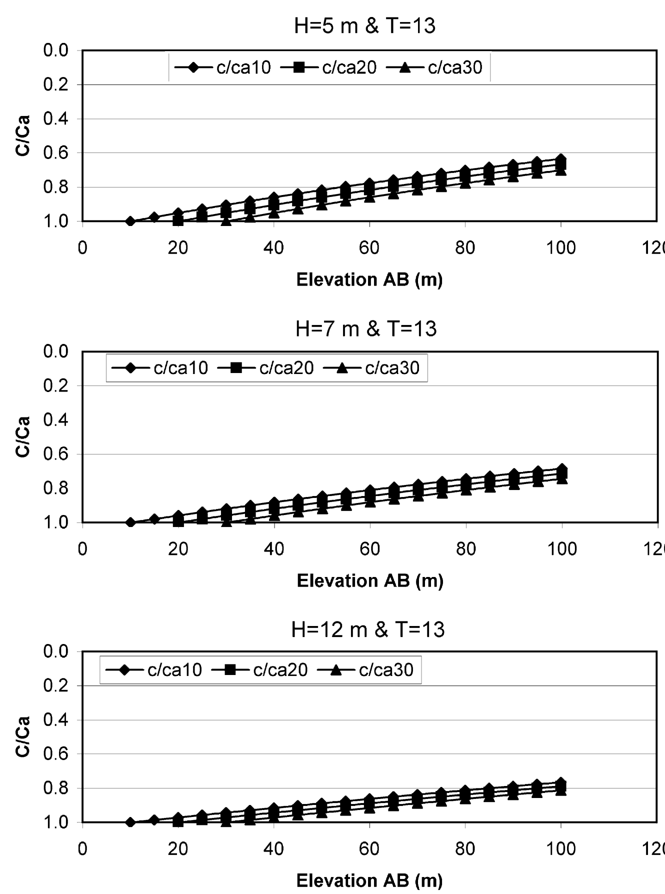

Fig. 11. Vertical concentration of nepheloid material (C/C_a) as a function of wave height and period during tropical storms and hurricanes and high current speeds.

resuspension of the nepheloid layer during all hurricane categories, but not during calm conditions. Of course, the nepheloid sediments will be carried or advected by prevailing currents as seen at other localities (Chang et al., 2001), thus reducing their impact to the FGB corals. These results suggest that shunting of drilling fluids from oil and gas activities to protect the FGB reefs works as designed. Two available observations suggest that impacts of nepheloid layer resuspension may not be significant: (1) no terrigenous clastic particles have been identified among the reef sediments (Rezak et al., 1983) and (2) sediment facies show a low percentage of noncarbonate material at the banks (Scanlon et al., 2005).

Finally, another hurricane impact factor is its capacity to induce fluxes of temperature and salinity across the shelf edge. Hamilton et al. (2000) found that, during storms near the DeSoto Canyon, tropical storms drove on- and offshore transport of heat and salt. These fluxes should bring nearshore and offshore water masses across the reefs, whose impacts need to be quantified. It is important to note that responses to storms vary spatially, i.e., at different places the fluxes were opposite and of variable magnitude. We examined the LATEX shelf's response to hurricanes by examining currents from the Texas Automated Buoys, Fig. 1 (see http://tabs.gerg.tamu.edu/Tglo/). Daily average surface currents at 10 buoys are shown in Fig. 12. Before the hurricane arrived, left panel, currents were variable in direction and speed, but mostly sluggish, $<0.3\ \mathrm{m\,s^{-1}}$. Between September 22 and 23, center panel, the flow started organizing in the downcoast, or toward Texas, especially near Louisiana, and the speed began to increase. The outer buoys captured stronger flows as they are closer to the hurricane. By September 23–24, right panel, the shelf flow was directed downcoast with an offshore component at speeds of 0.4–0.7 $\mathrm{m\,s^{-1}}$. This response is fairly typical since strong hurricane winds are directed downcoast as documented by Nowlin et al. (1998) and Bender et al. (2007). Pre-storm hydrographic conditions over the entire shelf reveal surface temperatures of 29–31 °C (plot not shown), with the highest temperatures near the shoreline. These conditions are warmer than average summer temperatures, which show surface temperatures around 29.5 °C in nearshore areas and about 28–30 °C near the bottom (Nowlin et al., 1998). During the hurricane, temperature data from buoys reveal that nearshore areas did not cool much, but waters over the FGB cooled the most (~2 °C), especially near the cap reefs. This temperature response suggests hurricane-induced upwelling, a common response to such systems. Average summer surface salinity across the shelf is about 28–36 with about 32 in nearshore areas and 36 by the FGB on shelf edge (Nowlin et al., 1998). The intense vertical mixing during hurricanes must have created a nearly homogenous water mass over the shelf, with temperatures near 29 °C and salinities between 28 and 36, which, coupled with offshore transport, help explain the warm temperatures and high salinity observed at the FGB after the storm. A plot of east–west and north–south currents (not shown) reveals that nearshore and offshore waters responded differently during Hurricane Rita. Nearshore, at TABS buoy R, the currents during Rita displayed a near steady alongshore component of $\sim 0.25\ \mathrm{m\,s^{-1}}$, but the north–south component showed oscillations of 0.3–0.5 $\mathrm{m\,s^{-1}}$. At TABS buoy N over the FGB, both velocity components during Rita exhibit

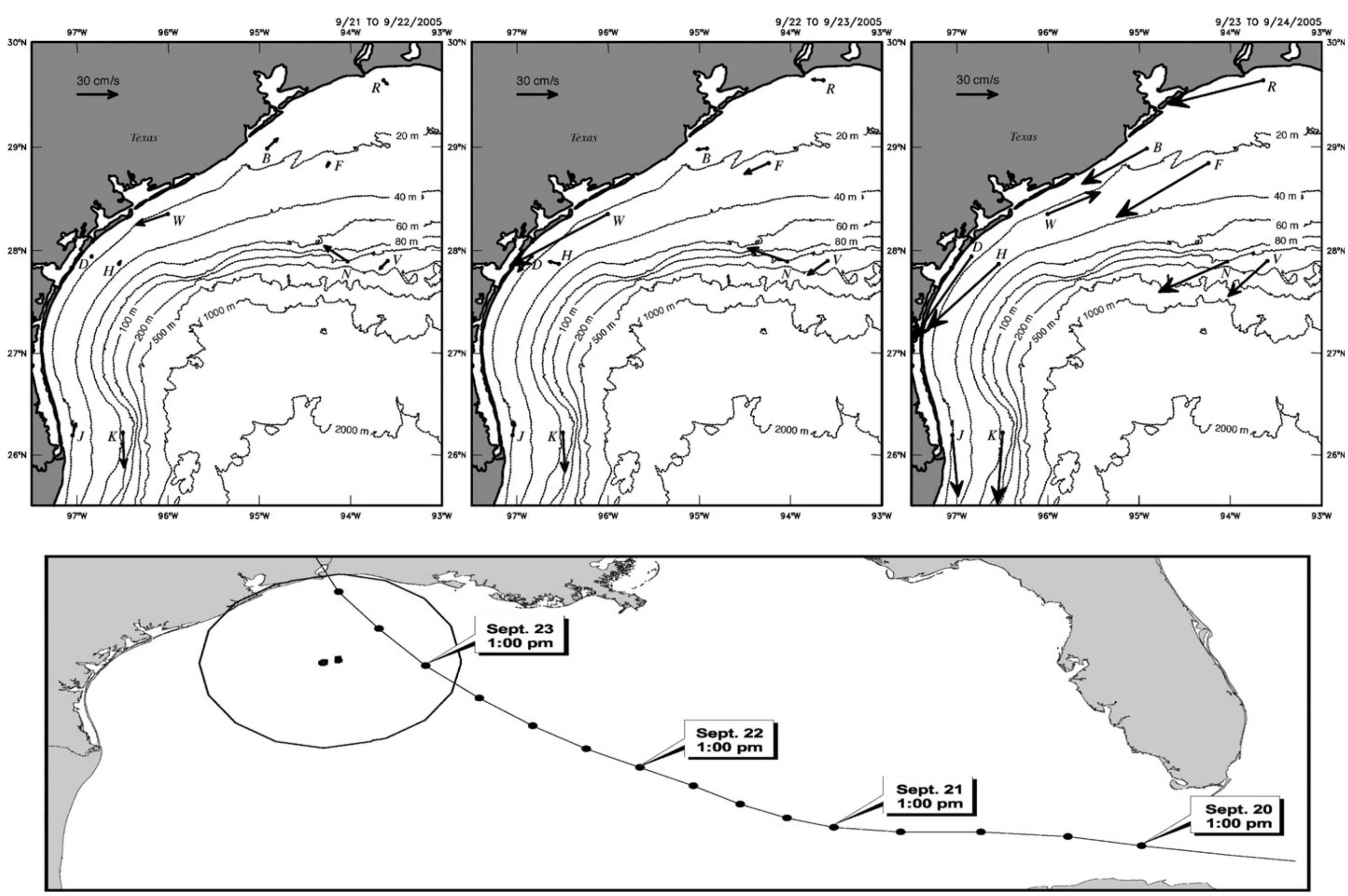

Fig. 12. Shelf current variations across the LATEX shelf from September 21 to 24 during Hurricane Rita in 2005. The lower panel shows positions of Hurricane Rita near noon local time during this time.

oscillations of about 0.2 m s^{-1} and are opposite with periods near 24 h. These current patterns suggest near inertial currents. These different responses of nearshore and shelf edge waters can be explained using the parameter U/c, where U is the hurricane translation speed and c the long wave speed. For Hurricane Rita, U was ~6–10 m s^{-1} and c ($=\sqrt{gh}$ for the well mixed water column at buoy R) was ~10 m s^{-1} since the water depth is 9.8 m in this nearshore area; then $U/c\sim1$. The finding that $U/c\sim1$ indicates that a near inertial trail should not have occurred. At buoy N, c is near 0.6 m s^{-1} given the stratification of the water at this site and $(U/c)\gg1$, and the trail of near inertial motions was observed. The advection of warm and salty waters from upstream of the FGB, solar heating, and oscillatory inertial motions at this site combine to help explain the temperatures above 30 °C and subsequent bleaching of the corals observed after Hurricane Rita at the FGB (Precht et al., 2008a). The oscillatory motions induced very little net transport, and these waters remained in the same area being heated by solar radiation. These conditions acted as an additional process of connecting nearshore areas with offshore reefs, as suggested by Deslarzes and Lugo-Fernández (2007), but in a very short time instead of a seasonal cycle.

4.4. Dispersal

Given that the tropical hurricane and coral spawning seasons in the Atlantic basin coincide (Gardner et al., 2005; Lugo-Fernández et al., 2001), it is conceivable that storms and hurricanes can aid coral dispersal, but the number of such observations is small. Below we explore how hurricanes could impact coral dispersal.

Review of previous works indicates that storms and hurricanes aid short-distance coral dispersal by fragmentation of corals, which are then dispersed by waves and currents. This mechanism constitutes self-seeding as fragments do not leave the reef site. Additionally, this mechanism seems applicable mostly to branching corals (Jackson, 1991), which are very susceptible to mechanical breakage by waves and currents. Massive corals, which are more resistant to breakage, could be displaced when dislodged by rolling, but one has to wonder if polyps survive such conditions and contribute to dispersal of these corals.

During a study of larval dispersal at the FGB, Lugo-Fernández et al. (2001) noted that tropical storms approaching Texas induced very rapid transit of drifters from US to Mexican waters along the inner shelf in the western gulf with displacements of 180–230 km at speeds of ~0.75 m s^{-1} (see their Figs. 4 and 5). They proposed that such storms could induce an exchange of larvae among reefs of southern Mexico and the FGB. A similar example occurred in September 1979, when a tropical depression hit southern Texas (Gundlach and Finkelstein, 1981) and satellite tracked drifters released in the western gulf also moved southward along the inner shelf at speeds of ~100 cm s^{-1} reaching near 20°N (Mountain et al., 1980). These observations strongly suggest that tropical storms and hurricanes in the western Gulf of Mexico have the potential to induce long-distance dispersal of larvae and affect connectivity of the FGB with Mexican reefs. The physical reason for such strong southward flow is twofold: (1) shallow shelf waters respond very fast to winds and (2) storm's winds flow counter-clockwise, which induce southward winds when a hurricane is traveling with the coast to their left or approaching the coast head-on. This arrangement is a common situation in the western gulf as the observed approach and contact distributions indicate.

The possibility of long-distance dispersal of coral larvae onto the FGB occurs when a storm or hurricane moves northeastward across the gulf or from the south. This possibility was demonstrated by Tropical Storm Josephine in 1996, which originated in the southwest gulf, pushed waters from the northeastern gulf and Florida areas, where the Middle Ground coral communities are, into the LATEX shelf (Ohlmann and Niiler, 2001). In this instance, the storm forced water westward along the shelf edge, which reached the FGB area in about 1 month, which is close to the competency period of larvae; see Fig. 11 in Lugo-Fernández (1998). Another possibility exists when storms approach the FGB area from the southeast, which is the most common direction of incidence. In this case, storms can push waters northwestward across the deep Gulf in conjunction with the strong Loop Current and reach the FGB in about 55 days along a route similar to that in Lugo-Fernández (2006). Precht et al. (2008b) hypothesized that this route could explain the recent recruitment of *A. palmata* in the FGB. Again, this travel time is close to the competency period of coral larvae. This route will bring coral larvae from reefs in the Campeche and Yucatan areas to the northwestern Gulf reefs and coral communities.

5. Summary

This study, unlike many previous works of storm–reef interaction, is not a forensic analysis of a particular event at the FGB. It is, however, an examination of potential impacts of tropical storms and hurricanes on these reefs based on well-accepted processes active during such events. The studied reefs were selected because of their relevance to the applied science communities on the Gulf of Mexico, but more so because these are submerged bank reefs located 200 km offshore at the boundary between neritic and oceanic waters. These reefs cap two topographic features and lie in the water column, unlike most Caribbean reefs, which are either at the seafloor near the shelf edge or near the surface of nearshore areas. Their geographic positions (latitude, longitude, and depth) place them away from the fresher and sediment laden waters generally occurring in the nearshore areas of this shelf; their vertical positions put these reefs over the seafloor, which at this location is an unsuitable habitat for coral reef growth. Thus, these reefs provide an excellent opportunity to study storm or hurricane effects without the confounding effects of nearshore factors such as runoff and sedimentation, or anthropogenic stresses. However, these reefs are not analogues of typical fringing-barrier Caribbean reefs because their coral growth depth (18–50 m) shields them from all impacts except the most infrequent hurricanes and they lack the typical Caribbean coral zonation.

The 100-year storm climatology developed for the FGB is a new result from this work. It shows that that the FGB has a 50% chance of a tropical storm coming within 200 km every year. But direct hits are less frequent, with a 17% chance every year or about one direct hit every 5–6 years. The climatology indicates that tropical storms and hurricanes affect these reefs anytime from May through November with a peak in August–September and mostly as tropical storms or Category 1 hurricanes, but can be as intense hurricanes also. The climatology also shows that these reefs are impacted from almost any direction, but they are most frequently impacted from the southeast or southwest, indicating that only Atlantic or gulf storms impact these reefs. Assuming little or no uplifting of the banks and on the basis of the sea-level curve for the Gulf of Mexico (Balsillie and Donoghue, 2004), these coral reefs should be at least 8000–9000 years old. This age suggest about 6000 instances of storm–FGB interactions or 1300 direct hits. Finally, this climatology reveals a cycle of tropical storm activity with a time scale of 30–40 years, similar to hurricane activity of the Atlantic basin. It is interesting to note that this time (25–40 years) is very similar to the recovery time generally observed for coral reefs and suggests that storms impart this time scale to the ecosystem.

The force analysis reveals that the hydrodynamics forces generated by these storms and hurricanes are not enough to cause breakage because most of the corals present at the FGB are not of the branching type and because of the water depths involved. However, as Madin (2005) shows, the forces could be enough to dislodge colonies. The analysis also revealed the possibility of hydrodynamic pruning occurring. The wave and current velocities are enough to resuspend large (3 cm) quartz particles. Although quartz particles of this dimension are not included in FGB sediments, particles of coral that are hydraulic equivalents impact colonies by acting as abrasive agents or projectiles. These effects have been observed at the FGB. Another result is the removal of sediments from these reefs as they are transported off-bank and onto the nearby seafloor. Because these reefs are at the shelf edge, the removed sediments would be lost from the shelf as well. Precht et al. (2008a) found evidence of these processes occurring at the FGB during Hurricane Rita. The wave and current speeds generated by intense storms are sufficient to resuspend sediment in the nepheloid layer and reach the coral reefs; however, advection, coupled with the settling velocities, most probably ensures that any impacts from these sediments are short lived. On a positive side, mixing induced by the storms can interrupt the summer high temperatures by upwelling and entrainment of deep waters and can ameliorate coral bleaching. This work has also found evidence suggesting that after the storms, nearshore waters can be transported toward these offshore reefs by the resulting hurricane-generated shelf circulation. These waters could be warm and sediment laden and could affect the optical parameters of these otherwise transparent waters; however the optical changes may not adversely impact the reefs. A sluggish and oscillatory circulation near the FGB, along with high solar radiation, could combine to raise temperatures above 30 °C after hurricanes to resume coral bleaching as was observed by Precht et al. (2008a). Finally, the coincidence of tropical hurricane and spawning seasons can help coral dispersion by inducing strong currents, which could transport larvae over longer distances and within the competency period to affect recruitment in other places. Additionally, these storms could increase the chance of recruitment from faraway reefs, thus increasing the genetic diversity of the FGB.

It is well known that shallow reefs tend to loose coral cover when impacted by intense hurricanes (e.g., Alvarez-Filip et al., 2009), but the climatology derived here shows that most storms affecting the FGB are tropical storms. Hence how much coral cover change has occurred at the FGB reefs because of these storms? Unfortunately, we have access only to 13 years of coral cover observations at the FGB, well short of the 25–40 years' cycle of storm activity observed. Fig. 13 shows coral cover for both the EFGB and WFGB reefs along with the number of storms affecting the FGB from 1992 through 2005. These data show that coral cover at both banks ranged from 35% to 65% with a mean of 50%. Statistically, mean coral cover and its variance are equal at both banks at the 98% confidence level. The data also suggest an increasing trend during the same interval. However, the linear positive trend was not significant at the EFGB, but it was significant at the 95% confidence level at the WFGB. Correlation between number of storms and coral cover was positive (0.36 at the EFGB and 0.61 for the WFGB) but this is a spurious result since it is well known that storms reduce, and not increase, coral cover. Thus, the correlation analysis was not pursued. Because the variance and means are similar between banks, the coral cover data were pooled by averaging observations from both banks. The correlation analysis indicates that the number of hurricanes is not the pertinent variable to study storm impacts. Review of recent

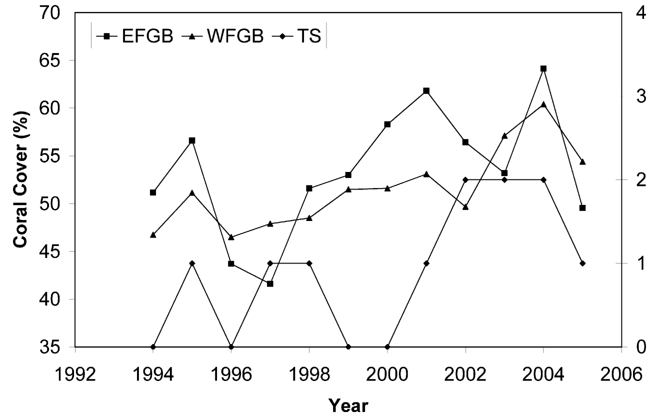

Fig. 13. Plot of FGB coral cover from 1992 to 2005 in the West Flower Garden Bank (WFGB) and the East Flower Garden Bank (EFGB) and number of storms (TS) contacting these reefs.

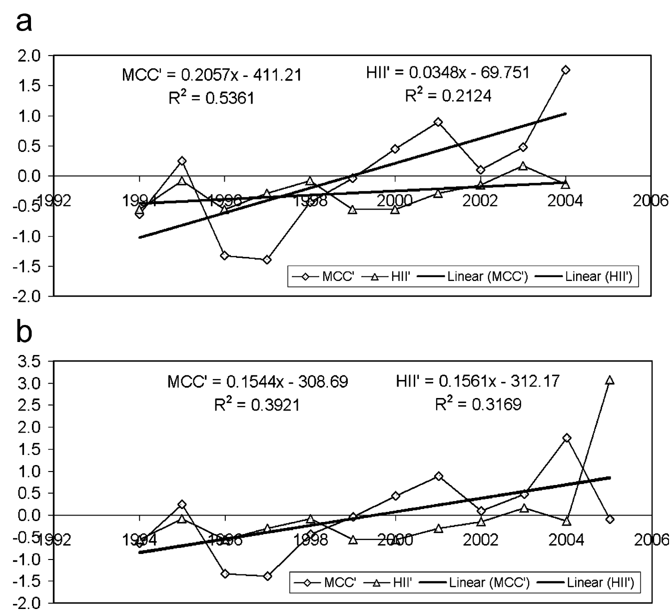

Fig. 14. Plot of transformed coral cover (MCC) and transformed hurricane intensity index (HII) at the FGB from 1992 to 2004 (a) and from 1992 to 2005 (b). The MCC and HII were transformed by subtracting the respective mean and dividing by the respective standard deviation of each series.

literature reveals that the hurricane intensity index (HII), defined as $(V_m/V_{0m})^2$, where V_m is the maximum wind speed in the hurricane and V_{0m} is a reference speed set to 33 m s^{-1} (Kantha, 2008), should be a better measure to study hurricane impacts. For a Category 1 hurricane HII equals exactly 1, HII is <1 during tropical storms, and HII is >1 for Category 2 and stronger hurricanes. In this study, the storm or hurricane wind speed measured inside the 200-km buffer and closest to the FGB was selected as V_m. We subtracted the mean and divided this difference by the standard deviations of both the pooled coral cover and HII (see results in Fig. 14). In Fig. 14a, coral cover up to 2004 shows a positive trend, while HII remains nearly leveled over the same period. Fig. 14b shows the coral cover and HII including 2005, and the last year represents a reduction of ca. 11% in coral cover induced by the jump of ~3 in HII. The observations of coral cover and HII in Fig. 14 are interpreted as follows: from 1994 to 2004, storm activity at the FGB was at tropical storm or lower intensity and HII is below average, and during this period coral cover exhibited a positive trend. Recall that coral mortality is high even in the absence of hurricanes (Hughes and Connell, 1999). In 2005, HII increased to ~3 due to Hurricane Rita and coral cover decreased markedly (~11%) in response. Note that the coral cover reduction of 11% is as large as the total increase during the years of low storm activity, ~18%. It is speculated that the reasons for the increase during low storm activity are (1) the type of coral present in the FGB, mostly massive instead of branching corals; (2) the depth, i.e., ~18–50 m, of these reefs, which tends to reduce hurricane effects; (3) these reefs tend to be self seeded; and (4) that their pre-hurricane health is relatively good given the low impact from nearshore runoff and anthropogenic stressors (Schmahl et al., 2008). Note that distance between storms and reef has not been considered in this analysis. On the basis of these results, it is apparent that the FGB coral reefs act as larvae centers, which can help colonization of other reefs. Their refugia role becomes more relevant under a climate change scenario, which should affect tropical fringing reefs more due to the expected increase in storm intensity due to a warmer climate. Further research on the correlation between MCC and HII is needed to verify it and to develop an index that includes other storm and reef aspects controlling impacts on coral reefs.

Acknowledgements

The authors appreciate the support of the US Department of the Interior, Minerals Management Service, Gulf of Mexico OCS Region during the preparation of this manuscript. The opinions expressed by the authors are their own and do not reflect the opinion or policy of the US Government. Thanks to Doctors Evans Waddell and Peter Hamilton of SAIC for helping with Fig. 12, Mr. James Sinclair of MMS for providing the coral cover data at the FGB, Dr. Harry H. Roberts of LSU, and an anonymous reviewer for helpful suggestions. Thanks to Mr. William Precht of NOAA for suggesting this work.

References

Alvarez-Filip, L., Millet-Encalad, M., Reyes-Bonilla, H., 2009. Impact of Hurricanes Emily and Wilma on the coral community of Cazumel Island, Mexico. Bull. Mar. Sci. 84 (3), 295–306.

Aronson, R.B., Precht, W.F., Murdoch, T.J.T., Robbart, M.L., 2005. Long-term persistence of coral assemblages on the Flower Garden Banks, northwestern Gulf of Mexico: implications for science and management. Gulf Mex. Sci. 23, 84–94.

Aronson, R.B., Precht, W.F., 2001. Evolutionary paleoecology of Caribbean coral reefs. In: Allmon, W.D., Bottjer, D.J. (Eds.), Evolutionary Paleoecology: The Ecological Context of Macroevolutionary Change. Columbia University Press, NY, pp. 171–233.

Balsillie, J.H., Donoghue, J.F., 2004. High resolution sea-level history for the Gulf of Mexico since the last glacial maximum. Florida Geological Survey Report of Investigations No. 103, Florida, USA.

Bender III, L.C., Guinasso Jr., N.L., Walpert, J.N., Lee III, L.L., Martin, R.D., Hetland, R.D., Baum, S.K., Howard, M.K., 2007. Development, operation, and results from the Texas Automated Buoy System. Gulf Mex. Sci. 25, 33–60.

Blanchon, P., Jones, B., Kalbfleisch, W., 1997. Anatomy of a fringing reef around Grand Cayman: Storm rubble, not coral framework. J. Sedimentat. Res. 67 (1), 1–16.

Boland, G.S., 1998. Spawning observations of the scleractinian coral *Colpophylia natans* in the northwest Gulf of Mexico. Gulf Mex. Sci. 16, 226–227.

Breaker, L.C., Burroughs, L.D., Culp, J.F., Guinasso Jr, N.L., Teboulle, R.L., Wong, C.R., 1994. The impact of Hurricane Andrew and the near-surface marine environment in the Bahamas and the Gulf of Mexico. Weather Forecast. 9, 542–556.

Bright, T.J., Kraemer, G.P., Minnery, G.A., Viada, S.T., 1984. Hermatypes of the Flower Garden Banks, northwestern Gulf of Mexico: a comparison to other western Atlantic reefs. Bull. Mar. Sci. 34, 461–476.

Bright, T.J., Pequegnat, L.H., 1974. Biota of the West Flower Garden Banks. Gulf Publishing Company, Book Division, TX.

Bythell, J.C., Hillis-Starr, Z.M., Rogers, C.S., 2000. Local variability but landscape stability in coral reef communities following repeated hurricanes impacts. Mar. Ecol. Prog. Ser. 93, 93–100.

Chang, E.K.M., Guo, Y., 2007. Is the number of North Atlantic tropical cyclones significantly underestimated prior to the availability of satellite observations? Geophys. Res. Lett. 34, doi:10.1029/2007GL030169.

Chang, G., Dickey, T., Williams III, A., 2001. Sediment resuspension over a continental shelf during Hurricanes Edouard and Hortense. J. Geophys. Res. 106 (C6), 9517–9531.

Chen, C., Reid, R.O., Nowlin, W.D., 1996. Near-inertial oscillations over the Texas–Louisiana shelf. J. Geophys. Res. 101 (C2), 3509–3524.

Dean, L., Emanuel, K.A., Chavas, D.R., 2009. On the size distribution of Atlantic tropical cyclones. Geophys. Res. Lett. 36, L1483, doi:10.1029/2009LG039051.

Denny, M.W., 1988. Biology and the Mechanics of the Wave-swept Environment. Princeton University Press, New Jersey.

Deslarzes, K.J.P., Lugo-Fernández, A., 2007. Influence of terrigenous runoff on offshore coral reefs: an example from the Flower Garden Banks, Gulf of Mexico. In: Aronson, R.B. (Ed.), Geological Approaches to Coral Reef Ecology: Placing the Current Crises in Historical Context. Springer Verlag, pp. 126–160.

Deslarzes, K.J.P., 1998. The Flower Garden Banks (Northwest Gulf of Mexico: environmental characteristics and human interaction. OCS Report MMS 98-0010, US Department of the Interior, Minerals Management Service, Gulf of Mexico OCS Region, New Orleans, LA.

DiMarco, S.F., Meza, E., Zhang, J., 2001. Estimating wave elevation from pressure using second-order nonlinear wave–wave interaction theory with applications to Hurricane Andrew. J. Coastal Res. 17, 658–671.

Dollar, S.J., 1982. Wave stress and coral community structure in Hawaii. Coral Reefs 1, 71–81.

Donnelly, J.P., Woodruff, J.D., 2007. Intense hurricane activity over the past 5000 years controlled by El Niño and the West African monsoon. Nature 447, 465–468.

Emanuel, K., Sundararajan, R., Williams, J., 2008. Hurricanes and global warming: results from downscaling IPCC AR4 simulations. Bull. Am. Meteorol. Soc. 89, 347–367.

Frank, W.M., 1977. The structure and energetics of the tropical cyclone I. storm structure. Mon. Weather Rev. 105, 1119–1135.

Gardner, J.V., Mayer, L.A., Hughes, C.J.E., Kleiner, A., 1998. High-resolution multibeam bathymetry of East and West Flower Gardens and Stetson Banks, Gulf of Mexico. Gulf Mex. Sci. 16, 131–143.

Gardner, T.A., Cote, I.M., Gill, J.A., Grant, A., Watkinson, A.R., 2005. Hurricanes and Caribbean coral reefs: impacts, recovery patterns, and role in long-term decline. Ecology 86, 174–184.

Gittings, S.R., 1998. Reef community stability on the Flower Garden Banks, Northwest Gulf of Mexico. Gulf Mex. Sci. 16, 161–169.

Gittings, S.R., Boland, G.S., Deslarzes, K.J.P., Combs, C.L., Holland, B.S., Bright, T.J., 1992a. Mass spawning and reproductive viability of reef corals at the East Flower Garden Bank, northwest Gulf of Mexico. Bull. Mar. Sci. 51, 420–428.

Gittings, S.R., Boland, G.S., Deslarzes, K.J.P., Hagman, D.K., Holland, B.S., 1992b. Long-term monitoring at the East and West Flower Garden Banks. OCS Study MMS 92-0006, US Department of the Interior, Minerals Management Service, Gulf of Mexico OCS Regional Office, New Orleans, LA.

Gittings, S.R., Boland, G.S., Merrit, C.R.B., Kendall, J.J., Deslarzes, K.J.P., Hart, J., 1994. Mass spawning by reef corals in the Gulf of Mexico and Caribbean Sea. Flower Gardens Fund Technical Series Report No. 94-03, The Flower Gardens Fund of the Gulf of Mexico Foundation.

Glynn, P.W., 1973. Ecology of a Caribbean coral reef, the *Porites* reef flat biotope—part 1: meteorology and hydrography. Mar. Biol. 20, 297–318.

Glynn, P., Almodóvar, L.R., Gonzalez, J.G., 1964. Effects of Hurricane Edith on marine life in La Parguera, Puerto Rico. Caribb. J. Sci. 74, 335–345.

Goldenberg, S.B., Landsea, C.W., Mestas-Nuñez, A.M., Gray, W.M., 2001. The recent increase in Atlantic hurricane activity: causes and implications. Science 20, 474–479.

Grauss, R.R., Macintyre, I.G., Herchenroder, B.E., 1984. Computer simulation of the reef zonation at Discovery Bay, Jamaica: hurricane disruption and long-term physical oceanographic controls. Coral Reefs 3, 59–68.

Gundlach, E.R., Finkelstein, K.J., 1981. Transport, distribution, and physical characteristics of the oil, in the IXTOC 1 oil spill. In: Hooper, C.H. (Ed.), The Federal Scientific Response. NOAA, pp. 41–73.

Hagman, D.K., Gittings, S.R., Deslarzes, K.J.P., 1998. Timing, species participation and environmental factors influencing annual mass spawning at the Flower Garden Banks (northwest Gulf of Mexico). Gulf Mex. Sci. 16, 170–187.

Hamilton, P., Berger, T.J., Singer, J.J., Waddell, E., Churchill, J.H., Leben, R.R., Lee, T.N., Sturges, W., 2000. Desoto Canyon eddy intrusion study, final report, vol. II: Technical report. OCS Study MMS 2000-080, US Department of the Interior, Minerals Management Service, Gulf of Mexico OCS Region, New Orleans, LA.

Harmelin-Vivien, M.L., 1994. The effects of storms and cyclones on coral reefs: a review. J. Coastal Res. 12, 211–231.

Harmelin-Vivien, M.L., Laboute, P., 1986. Catastrophic impact of hurricanes on atoll outer reef slopes in the Tuamotu (French Polynesia). Coral Reefs 5, 55–62.

Hernández-Ávila, M.L., Roberts, H.H., Rouse, L.J., 1977. Hurricane generated waves and coastal boulder rampart formation. In: Proceedings of the Third International Coral Reef Symposium, University of Miami, Florida, pp. 71–78.

Hughes, T.P., Connell, J.H., 1999. Multiple stressors on coral reef: a long-term perspective. Limnol. Oceanogr. 44, 932–940.

Jackson, J.B.C., 1991. Adaptation and diversity of reef corals. BioScience 41, 475–482.

Jarosz, E., Mitchell, D.A., Wang, D.W., Teague, W.J., 2007. Bottom-up determination of air–sea momentum exchange under a major tropical cyclone. Science 315, 1707–1709.

Kantha, L., 2008. Tropical cyclone destructive potential by integrated kinetic energy. Bull. Am. Meteorol. Soc. 89, 219–221.

Landsea, C.W., 2007. Counting Atlantic tropical cyclones back to 1900. EOS Trans. Am. Geophys. Union 88, 197–200.

Longman, M.W., 1981. A process approach to recognizing facies of reef complexes. In: Donald, F. Toomey (Ed.), European Fossil Reef Models. SEPM Special Publication No. 30, pp. 9–40.
Lugo, A.E., Rogers, C.S., Nixon, S.W., 2000. Hurricanes, coral reefs and rainforests: resistance, ruin and recovery in the Caribbean. Ambio 29, 106–114.
Lugo-Fernández, A., 1998. Ecological implications of hydrography and circulation to the Flower Garden Banks, northwest Gulf of Mexico. Gulf Mex. Sci. 16, 144–160.
Lugo-Fernández, A., 2006. Travel times of passive drifters from the western Caribbean to the Gulf of Mexico and Florida–Bahamas. Gulf Mex. Sci. 24, 61–67.
Lugo-Fernández, A., Hernández-Avila, M.L., Roberts, H.H., 1994. Wave energy distribution and hurricane effects on Margarita Reef, Southwestern Puerto Rico. Coral Reefs 13, 21–32.
Lugo-Fernández, A., Deslarzes, K.J.P., Price, J.M., Boland, G.S., Morin, M.V., 2001. Inferring probable dispersal of Flower Garden Banks coral larvae (Gulf of Mexico) using observed and simulated drifter trajectories. Cont. Shelf Res. 21, 47–67.
Madin, J.S., 2005. Mechanical limitations of reef corals during hydrodynamic disturbances. Coral Reefs 24, 630–635.
Manzanello, D.P., Brandt, M., Smith, T.B., Lirman, D., Hendee, J.C., Nemeth, R.S., 2007. Hurricanes benefit bleached corals. In: Proceedings of the National Academy of Sciences Early Edition, doi:10.1073/pnas.0701194104.
McClanahan, T., Polunin, N., Done, T., 2002. Ecological states and resilience of coral reefs. Conserv. Ecol. 6, 18, URL: 〈http://wwww.consecol.org/vol6/iss2/art18〉 (online).
McGrail, D.W., 1983. Flow, boundary layers, and suspended sediment at the Flower Garden Banks. In: Rezak, R., Bright. T.J., McGrail. D.W. (Eds.), Reefs and Banks of the Northwestern Gulf of Mexico: Their Geological, Biological, and Physical Dynamics. Final Report, Technical Report No. 83-1-T, US Depatment of the Interior, Minerals Management Service, Gulf of Mexico OCS Region, New Orleans, LA, pp. 141–230.
Mei, C.C., 1983. The Applied Dynamics of Ocean Surface Waves. John Wiley & Sons, New York, NY.
Mountain, D.G., Murray, J.J., Mooney, K.A., 1980. Operational use of satellite tracked buoys during the IXTOC 1 oil spill. In: Proceedings of the 16th Annual Marine Technology Society ALMAR Conference, Washington, DC, pp. 36–41.
Nowlin, W.D., Jochens, A.E., Reid, R.O., Dimarco, S.F., 1998. Texas–Louisiana shelf circulation and transport process study: synthesis report LATEX A. OCS Study MMS 98-0035 and MMS 98-0036, vols. I and II, US Department of the Interior, Minerals Management Service, Gulf of Mexico OCS Region, New Orleans, LA.
Ohlmann, J.C., Niiler, P.P., 2001. A two-dimensional response to a tropical storm on the Gulf of Mexico shelf. Journal of Marine Systems 29, 87–99.
Panchang, V.G., Li, D., 2006. Large waves in the Gulf of Mexico caused by Hurricane Ivan. Bull. Am. Meteorol. Soc. 87, 481–489.
Pandolfi, J.M., Jackson, J.B.C., 2007. Broad-scale patterns in Pleistocene coral reef communities from the Caribbean: implications for ecology and management. In: Aronson, R.B. (Ed.), Geological Approaches to Coral Reef Ecology: Placing the Current Crises in Historical Context. Springer-Verlag, pp. 201–236.
Pond, S., Pickard, G.L., 1983. Introductory Dynamical Oceanography 2nd ed. Pergamon Press, New York.
Precht, W.F., Aronson, R.B., Deslarzes, K.J.P., Robbart, M.L., Zimmer, B., Duncan, L., 2008a. Post-hurricane assessment at the East Flower Garden Bank long-term monitoring site: November 2005. OCS Study MMS 2008-019, US Department of the Interior, Minerals Management Service, Gulf of Mexico OCS Region, New Orleans, LA.
Precht, W.F., Aronson, R.B., Deslarzes, K.J.P., 2008b. Back to the future: Elkhorn coral returns to Texas reefs after 6000-year hiatus. In: McKay, M., Nides. J. (Eds.), Proceedings of the 24th Gulf of Mexico Information Transfer Meeting, January 2007, US Department of the Interior, Minerals Management Service, Gulf of Mexico OCS Region, New Orleans, LA, OCS Study MMS 2008-012, pp. 376–377.
Rezak, R., Bright, T.J., McGrail, D.W., 1985. Reefs and Banks of the Northwestern Gulf of Mexico: Their Geological, Biological, and Physical Dynamics. John Wiley and Sons, New York, NY.
Rezak, R., Gittings, S.R., Bright, T.J., 1990. Biotic assemblages and ecological controls on reefs and banks of the northwest Gulf of Mexico. Am. Zool. 30, 23–35.
Rezak, R., Bright, T.J., McGrail, D.W., 1983. Reefs and banks of the northwestern Gulf of Mexico: their geological, biological, and physical dynamics. Final Technical Report No. 83-1-T, Texas A&M University, USA.
Riegel, B., 2007. Extreme climatic events and coral reefs: how much short-term threat from global change. In: Aronson, R.B. (Ed.), Geological Approaches to Coral Reef Ecology: Placing the Current Crises in Historical Context. Springer-Verlag, pp. 315–341.
Rogers, C.S., 1993. Hurricanes and coral reefs: the intermediate disturbance hypothesis revisited. Coral Reefs 12, 127–137.
Scanlon, K.M., Ackerman, S.D., Rozycki, J.E., 2005. Sedimentary environments of east and west Flower Garden Banks area. Gulf Mex. Sci. 23, 115–123.
Schmahl, G.P., Hickerson, E.L., Precht, W.F., 2008. Biology and ecology of coral reefs and coral communities in the Flower Garden banks Region, northwestern Gulf of Mexico. In: Riegl, B.M., Dodge, R.E. (Eds.), Coral Reefs of the USA. Springer Science, pp. 221–261.
Scoffin, T.P., 1993. The geological effects of hurricanes on coral reefs and the interpretation of storm deposits. Coral Reefs 12, 203–221.
Shay, L.K., Elsberry, R.L., 1987. Near-inertial ocean current response to Hurricane Frederic. J. Phys. Oceanogr. 17, 1249–1269.
Simpson, R.H., Riehl, H., 1981. The Hurricane and its Impact. Louisiana State University Press, Baton Rouge, LA.
Sorokin, Y.I., 1995. Coral Reef Ecology. Springer-Verlag, Heidelberg.
Sosik, H., Green, R., Pegau, W., Roesler, C., 2001. Temporal and vertical variability in optical properties of New England shelf waters during late summer and spring. J. Geophys. Res. 106 (C5), 9455–9472.
Stoddart, D.R., 1962. Catastrophic storm effects on the British Honduras reefs and cays. Nature 196, 512–515.
Stoddart, D.R., 1969. Ecology and morphology of recent coral reefs. Biol. Rev. 44, 433–498.
Treml, E., Colgan, M., Keevican, M., 1997. Hurricane disturbance and coral reef development: a geographical information system (GIS) analysis of 501 years of hurricane data from the Lesser Antilles. In: Proceedings of the Eighth International Coral Reef Symposium, vol. 1, pp. 541–546.
US Department of the Army, Corps of Engineers, 1984. Shore Protection Manual, fourth ed.
Van Veghel, M.L.J., Hoetjes, P., 1995. Effects of tropical storm Bret on Curacao reefs. Bull. Mar. Sci. 56, 692–694.
Van Woesik, R., De Vantier, L.M., Glazebrook, J.S., 1995. Effects of cyclone Joy on nearshore coral communities of the Great Barrier Reef. Mar. Ecol. Prog. Series 128, 261–270.
Wang, D.W., Mitchell, D.A., Teague, W.J., Jarosz, E., Hulbert, M.S., 2005. Extreme waves under Hurricane Ivan. Science 309, 896.
Williams, W.J., Beardsley, R.C., Irish, J.D., Smith, P.C., Limeburner, R., 2001. The response of Georges Bank to the passage of Hurricane Edouard. Deep Sea Research Part II: topical studies in oceanography 48, 179–197.
Woodley, J.D., 1992. The incidence of hurricanes on the north coast of Jamaica since 1870: are the classic reef descriptions atypical? Hydrobiologia 247, 133–138.
Woodley, J.D., et al., 1981. Hurricane Allen's impact on Jamaican coral reefs. Science 214, 749–755.
Zedler, S.E., Dickey, T.D., Doney, S.C., Price, J.F., Yu, X., Mellor, G.L., 2002. Analyses and simulations of the upper ocean's response to Hurricane Felix at the Bermuda testbed mooring site: 13–23 August 1995. J. Geophys. Res. 107 (C12), doi:10.1029/2001JC000969.